2012

Attachment of Escherichia coli to poly(dimethylsiloxane) irradiated at 254NM

Alisa Townsend

ATTACHMENT OF *ESCHERICHIA COLI* TO POLY(DIMETHYLSILOXANE) IRRADIATED AT 254 NM

BY

ALISA TOWNSEND

A THESIS

Submitted in partial fulfillment of the requirements
for the degree of Master of Science in Chemistry
in
The Department of Chemistry
to
The School of Graduate Studies
of
The University of Alabama in Huntsville

HUNTSVILLE, ALABAMA
2012

In presenting this thesis in partial fulfillment of the requirements for a master's degree from The University of Alabama in Huntsville, I agree that the Library of this University shall make it freely available for inspection. I further agree that permission for extensive copying for scholarly purposes may be granted by my advisor or in his/her absence, by the Chair of the Department or the Dean of the School of Graduate Studies. It is also understood that due recognition shall be given to me and to The University of Alabama in Huntsville in any scholarly use which may be made of any material in this thesis.

Alisa Townsend
(Student Signature)

8/20/12
(Date)

THESIS APPROVAL FORM

Submitted by Alisa Townsend in partial fulfillment of the requirements for the degree of Master of Science in Chemistry and accepted on behalf of the Faculty of the School of Graduate Studies by the thesis committee.

We, the undersigned members of the Graduate Faculty of The University of Alabama in Huntsville, certify that we have advised and/or supervised the candidate of the work described in this thesis. We further certify that we have reviewed the thesis manuscript and approve it in partial fulfillment of the requirements for the degree of Master of Science in Chemistry.

Dr. Emanuel Waddell	8/18/2012 (Date)	Committee Chair
Dr. Luis Rogelio Cruz-Vera	8/20/2012 (Date)	
Dr. Robert McFeeters	8/20/12 (Date)	
Dr. Carmen Scholz	8/17/12 (Date)	
Dr. William Setzer	8-20-12 (Date)	Department Chair
Dr. John Fix	8/20/12 (Date)	College Dean
Dr. Rhonda Gaede	8/28/12 (Date)	Graduate Dean

ABSTRACT

School of Graduate Studies
The University of Alabama in Huntsville

Degree Masters of Science in Chemistry College/Dept. Science/Chemistry

Name of Candidate Alisa Townsend

Title Attachment of *Escherichia coli* to Poly(dimethylsiloxane) Irradiated at 254 nm

The purpose of this research was to determine a method to attach *Escherichia coli* to poly(dimethylsiloxane) irradiated at 254 nm. By determining a method for attachment, it can be used to pattern the *E. coli* cells which can ultimately be used for creation of biosensors or for bacterial studies. For attachment, an *E. coli* culture was grown in M9 media to an optical density of 0.5 – 0.7, and 10 mL of culture was poured into a Falcon™ tube. The irradiated PDMS was placed in the cell culture for one hour, removed, rinsed with deionized water, and dried with nitrogen. It was determined that the most bacterial attachment occurred at a pH of 2. The amount of irradiation time was also varied, but it was determined that there was roughly the same amount of attachment at all irradiation times. There was a pH dependence on the attachment of *E. coli* to native PDMS with attachment only seen at an acidic pH. Also, ATR-FTIR was performed on samples placed in media at different pH and different forms of M9 media, but the spectra showed either the native PDMS spectra or spectra of irradiated PDMS with a slight decrease in the carbonyl peak. To verify that carboxylic acids were present on the surface before and after being placed in media a methylene blue experiment was performed. The data showed that carboxylic acids were present. It is theorized that the *E. coli* are attaching to the native and irradiated PDMS via an electrostatic interaction.

Abstract Approval: Committee Chair

Dr. Emanuel Waddell

Department Chair

Dr. William Setzer

Graduate Dean

Rhonda Kay Gaede 8/28/12

Dr. Rhonda Gaede

ACKNOWLEDGEMENTS

This journey has been long and demanding, but it would not have been possible without many people that have helped me along the way. First, I would like to thank my advisor Dr. Emanuel Waddell for all of his support, guidance, and encouragement. He was available when I need guidance on what direction to go next for my research, and encouraging when things seemed to be falling apart. Next, I would like to thank the members on my committee, Dr. Robert McFeeters, Dr. Carmen Scholz, and Dr. Luis Rogelio Cruz-Vera, for their support throughout my research and writing process. Also, I am grateful to Dr. McFeeters for the BL-21 *E. coli* and the use of his lab, and Dr. Cruz-Vera for the W3110 *E. coli.*

I am grateful to members of Dr. McFeeters laboratory including Kasey Taylor, Morgan Gilbert, Mary Hames, and Dr. Hana McFeeters. At the beginning when I was learning the techniques for growing *E. coli*, they were always there to help and give me advice on what to do. They kept telling me that the *E. coli* grow on their own time, not mine.

All of my results were viewed using a laser scanning confocal microscope, so I would like to thank Connie Hajjar for teaching me how to use and understand it. She was always available when I needed help.

Lastly, I am grateful for Jason Bruce, Diana Lechuga, and my parents for their personal support and encouragement throughout these past two years.

TABLE OF CONTENTS

Page

LIST OF FIGURES

LIST OF SYMBOLS

Symbol	Definition
ω	omega
A	absorbance
c	concentration
ℓ	path length
ε	molar absorptivity
θ	contact angle
γ_{SL}	solid liquid interfacial tension
γ_{SV}	solid vapor interfacial tension
γ_{LV}	liquid vapor interfacial tension
w_{SLV}	work of adhesion
$\gamma_{s/o}$	solid surface tension in a vacuum
$\gamma_{s/l}$	solid liquid interfacial tension
$\gamma_{s/v}$	solid vapor interfacial tension
$\pi_{s/l}$	spreading pressure of solid liquid interface
$\pi_{s/v}$	spreading pressure of solid vapor interface
Å	Angstrom
OD	optical density
PI	propidium iodide
PDMS	poly(dimethylsiloxane)
PBS	phosphate buffered solution
LB	Luria-Bertani

CHAPTER 1

INTRODUCTION

1.1 Cell Patterning

Cell patterning is a process where bacterial or mammalian cells are attached to substrates such as polymers in a defined pattern [1]. The ability to control the location of cellular attachment allows for multiple applications of this type of research including biosensors [2-5], tissue engineering [6-7], and biological studies to determine cell-surface and cell-to-cell interactions [8-10] to name a few. Biosensors with cells in a controlled location can be used to determine the response of cells to environmental and chemical conditions as well as drugs and disease conditions [1,11]. Tissue engineering is the creation of organized structures for whole tissues or creation of organs [1]. Cell patterning research can also help determine how mammalian and bacterial cells interact with surfaces at an interface. This type of research allows mechanisms and specific conditions of cell-to-cell and cell-surface interactions to be determined because cells can be placed into confined areas to monitor cell proliferation, movement, differentiation, and death [1,12]. Patterning of cells can be accomplished on many different types of surfaces depending on the information needed to be attained and what materials are available.

These substrates include silicon [13], gold [14], glass [15], poly(methylmethacrylate) [16], polystyrene [17], poly(ethylene terephthalate) [18], and poly(dimethylsiloxane), PDMS [19]. The method of attachment for cell patterning can also vary with information needed and what is available to the researcher. The most common technique used is microcontact printing of self-assembled monolayers (SAMs) to pattern extracellular matrix proteins for mammalian cells' attachment. Other techniques include UV irradiation, plasma treatment, and wet chemistry

Microcontact printing (μCP) is a soft lithography technique where a pattern is transferred to a substrate using a stamp. The most important aspect of this technique is the contact between the stamp and the substrate [20]. The stamp is created from a master with the needed pattern. Typically, the stamp is formed by casting PDMS onto a master (silicon or metal), and once the stamp is cured and removed, it is placed in a solution of molecules that can be transferred to the desired substrate [21]. When microcontact printing is used for cell patterning, SAMs are always the "ink" being transferred to the substrate [20]. Once the SAMs have been transferred to the surface, a second type of SAM can also be patterned on the surface in the open regions by soaking it in a solution containing the second SAMs. A schematic of μCP using SAMs can be seen in figure 1.1. The advantages of μCP include the ability to reuse the stamp multiple times, straightforward transfer techniques, minimization of material waste, and the technique can be used for two-dimensional and/or quasi-three-dimensional surfaces [20].

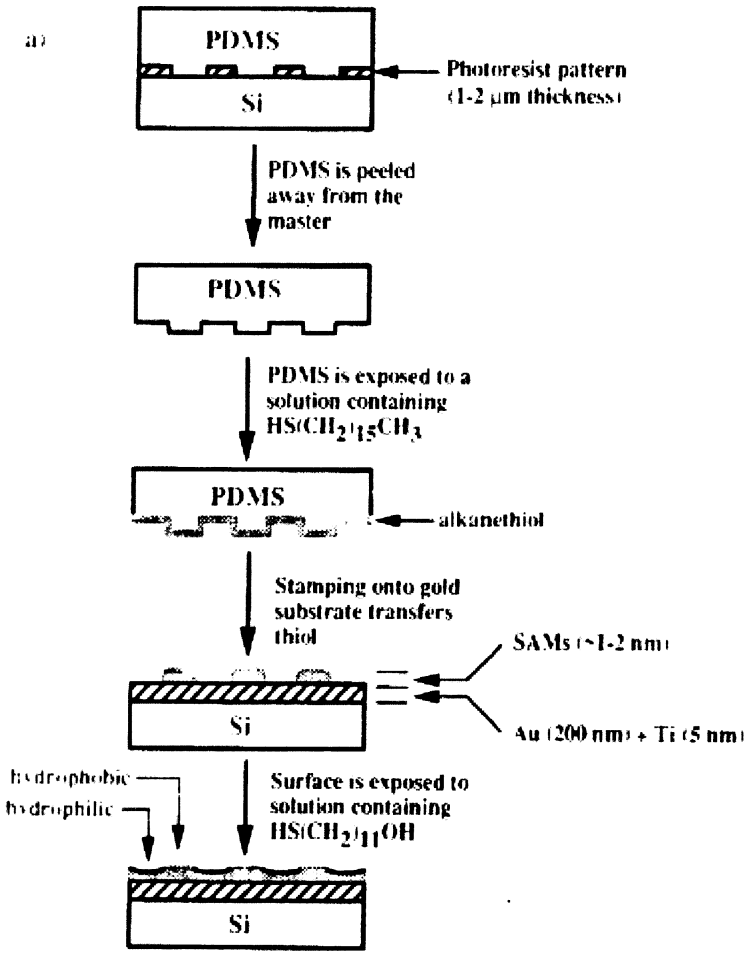

Figure 1.1 Schematic of microcontact printing and the creation of self-assembled monolayers on a surface containing adsorbed gold [21].

Self-assembled monolayers (SAMs) consist of long-chain alkanethiolates adsorbed onto gold or alkylsiloxanes on hydroxylated surfaces creating an organic surface [8]. The first research investigating long-chain alkyl disulfides and alkanethiols on gold surfaces came in the 1980s by Nuzzo and Allara [23] as well as Porter, Bright, and colleagues [24]. Alkanethiols are composed of $CH_3(CH_2)_nSH$ which is abbreviated as C_nSH. Another type of alkanethiolate is the ω-functionalized alkanethiol with the

structure of XC_nSH where X can be $-CH_3$, –COOH, –OH, or other terminal groups. The ω-functionalized alkanethiol is the most commonly used SAM since it is easily synthesized and easily functionalized with the needed surface characteristics [22, 25, 26]. The thiol group of the alkanethiols creates highly organized single layers of SAMs that are reproducible because there is a strong affinity of the thiol group for gold [22]. Alkylsiloxanes occur from the reaction of a hydroxylated surface and an alkyltrichlorosilane solution creating a cross-linked network of siloxanes [28-30]. The cross-linking occurs when the siloxane groups condense with water and surface hydroxyl groups. This class of SAMs is thermally more stable than alkanethiolates, but is limited in the terminal end group functionalization. The structure of alkanethiols and alkanesiloxanes are depicted in figure 1.1. Both classes of SAMs are stable in air or in a solution of water or ethanol for months, and the SAMs can desorb at temperatures greater than 70°C or UV irradiation in the presence of oxygen [8].

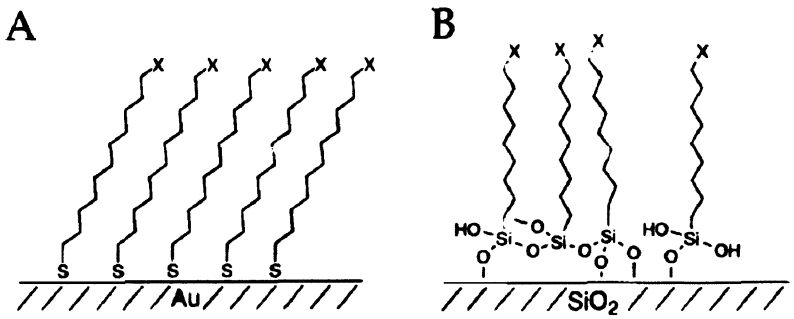

Figure 1.2 The structural and attachment differences between alkanethiolates (A) and alkylsiloxanes (B) [8].

The preparation of alkanethiols occurs by evaporating gold onto a flat substrate, then either exposing the gold surface to an alkanethiol solution or use μCP to pattern one type of SAM. The alkanethiol adsorbs onto the gold with a loss of the thiol hydrogen. The bond created between the SAM and gold is covalent with minimal polarity. The structure of a SAM with $n > 11$ consist of the chains being trans-extended and tilted vertically at a 30° angle, and if $n < 10$ there is less order in the chains [22]. For functionalized terminal groups, alkanethiols have possible steric constraints due to the terminal group causing the chains to pack differently and not align correctly; however, the surface density of SAMs changes which can prove to be useful [22, 27]. The advantages of SAMs include preparing the alkanethiol or alkanesiloxanes structures by synthesizing the design from basic organic molecules, very small quantities of organic materials needed, direct preparation of organic surfaces, easy characterization, and they can be used on large, heterogeneous, and non-planar substrates [22].

When SAMs are used for cell patterning, a protein is attached to the end functional group which provides a point of attachment for the cells. The most common type of protein used is typically an extracellular matrix protein including fibronectin, fibrinogen, collagen, and streptavidin [19, 31, 32]. Extracellular matrix proteins are a biological matrix made of insoluble proteins, glycoaminoglycans, peptides, and carbohydrate ligands [33]. M. Mrksich and colleagues used μCP to pattern SAMs for the attachment of bovine capillary endothelial cells on glass coverslips. The glass coverslip was first patterned using a stamp containing a hexadecanethiol which was then soaked in a solution of tri(ethylene glycol)-terminated alkanethiol. Once the glass coverslip was patterned, it was placed in a fibronectin solution which caused the extracellular matrix

protein to attach to the hydrophobic methyl group of hexadecanethiol. The mammalian cells attached to the fibronectin, but did not attach to the ethylene glycol groups which resist protein and cellular attachment [34]. K. Leong and colleagues patterned single mammalian cells in microwells using an alkanethiolate SAM with an aldehyde terminal group for collagen to attach. The SAMs were adsorbed onto the gold be immersing the PDMS substrate in a solution of (10-mercaptomethyl-9-anthyl)(4-aldehydepheyl) acetylene also called MMAAPA. The collagen was attached to the aldehyde of the MMAAPA through a covalent attachment between the amine groups. Only a single mammalian cell was found in each microwell and no cell attachment was found on the native PDMS surface [12]. Cerf et al. patterned octadecyltrichlorosilane which resists cell and protein attachment, and deposited streptavidin onto the other areas of the substrate for cell attachment [32]. These researchers used *E. coli* instead of mammalian cells, and were able to attach the *E. coli* to the streptavidin area of the substrate through a biotin-streptavidin bond [32]. S. Rozhok and colleagues patterned *E. coli* in microarrays. They adsorbed SAMs consisting of 16-mercaptohexadecanoic acid and 11-mercapto-1-undecanol onto gold, and then poly-L-lysine was attached to the SAMs for *E. coli* attachment. The *E. coli* only attached to the poly-L-lysine and not to the passivated area covered in 11-mercaptoundecyl-penta(ethylene glycol). This group also showed that the *E. coli* can attach to goat and rabbit anti-*E.coli* polyclonal antibodies, and rabbit *E. coli* anti-lipopolysaccharide antibody [35]. The above examples provide a concise literature review of cell patterning using self-assembled monolayers.

Other techniques used to pattern cells include plasma treatment, UV irradiation, and wet chemistry. Plasma treatment is useful for converting a hydrophobic surface to a

hydrophilic one. Frimate and coworkers stenciled a PDMS surface using plasma treatment [36]. A stencil covered the PDMS during the treatment such that the plasma would create a hydrophilic pattern on the surface. This group used ten different mammalian cell lines for cell attachment, and after an incubation period, the cells attached to the hydrophilic area of the PDMS created by the stencil [36]. UV irradiation can also be used to modify substrates for cell attachment. According to Gan and coworkers, mammalian cells can be attached to a PDMS substrate that has been irradiated at 172 nm [37]. The pattern for attachment was created by placing a stencil over the PDMS substrate during irradiation allowing only certain areas to be irradiated creating different properties on the surface [37].

Wet chemistry is chemistry done in the liquid phase, and it can also be used to pattern a substrate surface. For example, Hou and colleagues used this technique with extracellular matrix proteins to pattern mammalian cells. They used a copper grid to cover the PDMS surface, and immersed it in a solution of type II hydrophobin which was followed by immersing it in a solution of collagen. The modified PDMS substrate was inoculated with the mammalian cells which were shown to attach only to the extracellular matrix proteins [19]. Lastly, an adhesive was used to pattern mammalian cells as demonstrated by L. Tang and coworkers [11]. The PDMS was first plasma treated silanized with mercaptosilane, coated with the adhesive, exposed to UV irradiation at 365 nm using a stencil, cleaned by immersing in isopropyl alcohol and sonicating, and then post-cured with UV light. The mammalian cells were shown to attach to where the adhesive had been cured [11].

1.2 *Escherichia coli*

E. coli are considered a model organism, because it is one of the most understood living organism in the world [38]. It was first discovered in 1885 by Theodor Escherich who found it in the intestinal flora of an infant. He named it *Bacterium coli commune* [39]. *E. coli* have been used to study many different aspects of biology including bacterial physiology, determination of biochemical pathways, bacterial viruses, genetics, gene expression regulation, and protein synthesis. More recently it has been used for genetic engineering and production of commercial proteins. *E. coli* are very small rod shaped bacteria with dimensions of roughly 2.5 μm by 0.8 μm, and can be seen in figure 1.3. They have a three-layered cell wall encasing cytoplasm which does not contain a nucleus, organelles, or cytoskeletal elements. The cell wall does contain external organelles, pili which are thin straight filaments and flagella which are long thick helical filaments. The pili allow the bacteria to attach to surfaces, and flagella allow bacterial mobility [38].

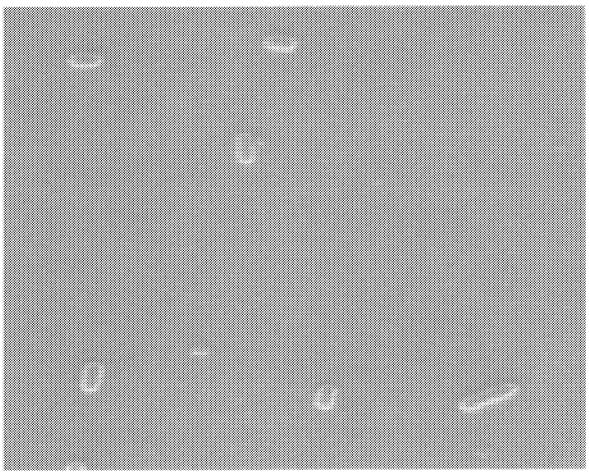

Figure 1.3 Scanning electron microscope image of *E. coli* attached to PDMS irradiated at 254 nm.

The movement of *E. coli* via a swimming motion is accomplished using flagella which function using a reversible rotary motor powered by a proton flux. *E. coli* can move in one of two ways: run or tumble. A run is when the bacterium goes straight in any one direction, and a tumble is when it has irregular movement in many random directions. The average time of a run is one second where a tumble averages about 0.1 seconds. The direction of movement is determined by cell wall receptors which count the molecules in the environment around the bacterium. If favorable components are found during a run, the movement is extended until a negative environment is found at which point it will begin to tumble for a few seconds before changing directions [38].

The *E. coli* membrane consists of an inner and outer membrane with peptidoglycan in-between which can be seen in figure 1.4. The outer membrane consists of intermembrane proteins and lipopolysaccharides (LPS). LPS are comprised of an inner and outer core and an O-antigen repeat which are composed of polysaccharide molecules. The exact make-up of the LPS will vary with each strain of *E. coli* [40, 41]. Peptidoglycan in gram-negative bacteria like *E. coli* includes partially cross-linked peptide chains and a backbone of muramic acid and glucosamine depicted in figure 1.5. The structure of muramic acid and glucosamine can be seen in figure 1.4. The purpose of this structure is for cell shape and protection [42].

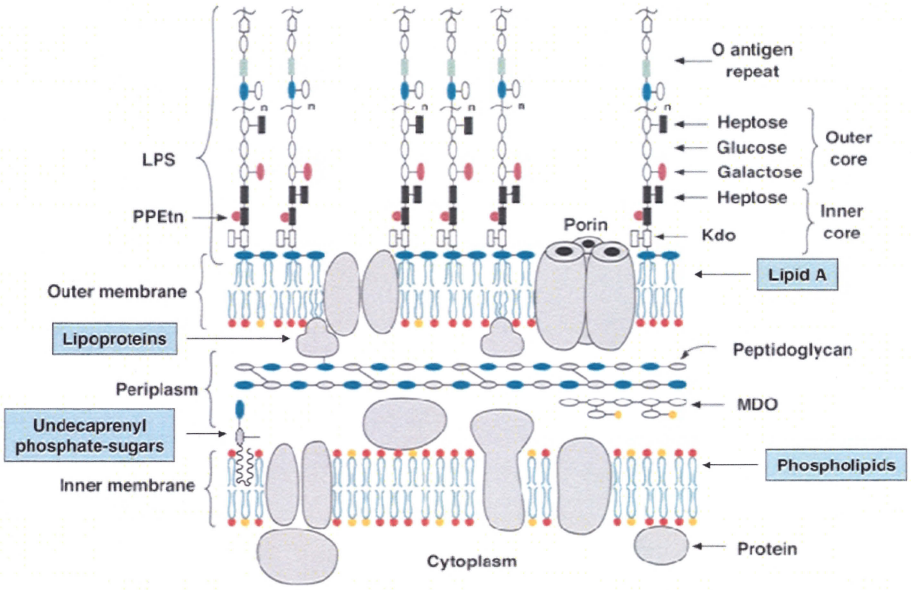

Figure 1.4 Schematic of the *E. coli* membrane taken from Raetz et al. [40].

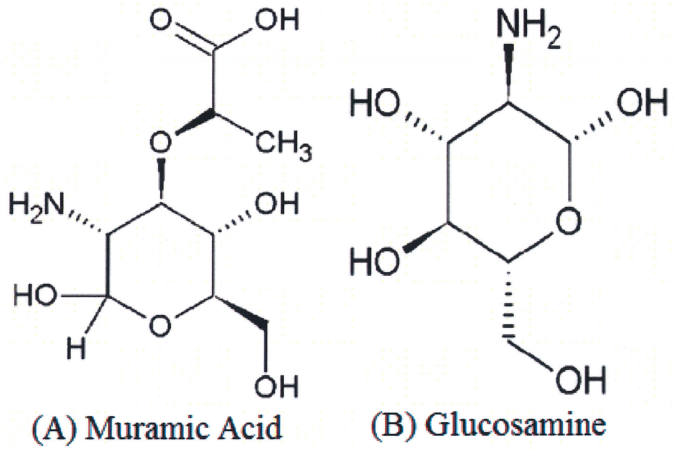

Figure 1.5 Structure of Muramic acid (A) and Glucosmine (B) which are found in peptidoglycan backbone.

E. coli are able to grow in various media including Luria-Bertani media consisting of tryptone, yeast extract, and sodium chloride as well as M9 minimal media containing sodium and potassium phosphates, glucose, vitamins, and salts. They are found in the lower intestines of warm-blooded animals, water, sediment, and soil. During growth, the bacterium grows in length, and then divides into two bacteria which are identical. *E. coli* bacteria only have one chromosome (haploid). All the DNA molecules are the same except when mutations occur; which do so at a rate of one per one million per generation. The bacteria are able to grow with oxygen (aerobic) or without oxygen (anaerobic), but prefer aerobic. Most people associate *E. coli* with the pathogenic variety that cause urinary tract infections, diarrheal diseases, and even death; however, most strains of *E. coli* are not extremely harmful. For example, the *E. coli* found in the gut of humans are capable of preventing yeast and fungal growth which are more harmful than *E. coli.*

The adhesion of bacteria to polymer and glass surfaces has been researched, and it has been determined that the following factors affect adhesion: environment, hydrophobicity, surface charge, surface roughness, and acid-base behavior [31, 43-45]. The environment of a bacterium can be a diversity of variables including temperature, exposure time, bacterial concentration, surface treatments, electrolyte concentrations [46, 47], and pH [46, 48, 49, 31]. These variables affect the interaction by modifying the surface characteristics of the substrate or bacteria. Hydrophobicity and hydrophilicity are terms used when considering the structure of water at a surface. A surface is hydrophobic when the water molecules do not hydrogen bond to it and are less ordered compared to a hydrophilic surface which will have hydrogen bonds between the water molecules and the surface as well as an ordered structure. These terms can be applied to

both bacterial surfaces and substrate surfaces. The hydrophobicity or hydrophilicity of bacteria is determined by the species, growth medium, bacterial age, and the outer membrane structure. It has been determined that hydrophobic bacteria will attach better to hydrophobic surfaces [31, 50], and hydrophilic bacteria will more likely attach to hydrophilic surfaces [31, 51, 52]. Surface hydrophobicity and hydrophilicity are primarily determined by surface chemistry. The surface charge on bacteria can also affect adhesion and varies depending on the species, growth medium, bacterial age, and the outer membrane structure [31]. The surface charge and hydrophobic or hydrophilic nature of the bacteria and surface can affect their interaction, and both characteristics can be incorporated into the acid base behavior of the surface and bacteria. An electrostatic force occurs when there is a net charge distribution on the surface and bacteria. Also, there are interactions involving permanent dipoles and induced dipoles. The acid-base interaction involves electric charge transfer between the bacteria and surface, ionic bonds, covalent bonds, or hydrogen bonds. According to Speranza and colleagues, the bacterial and surface interaction is a competition between water, positive charged ions, negative charged ions, outer membrane charges, and acidic/basic areas on the substrate surface which shows there is an acid-base interaction involved in bacterial adhesion with polymers [45]. Lastly, surface roughness has been researched to see its effect on bacterial adhesion. The roughness of a substrate is measured based on the distance between the peak and valley area of a surface but does not include morphological formations [31]. The research group of Baker and coworkers determined that bacterial adhesion occur on rougher surfaces because there is increased surface area, and the depressions are more advantageous for adhesion [53]. The theory of attachment due to

surface roughness is referred to as attachment point theory and states that bacteria will attach to a surface if the bacteria are on a smaller scale than the roughness of the surface due to the existence of many points for attachment [54-57]. Baker tested one strain from *E. coli, Staphylococcus aureus*, and *Pseudomonas Aeruginosa* to determine if there was a difference in attachment proclivity between the strains based on a smooth and rough glass slide. *E. coli* and *P. aeruginosa* were found to be hydrophilic and *S. aureus* hydrophobic. The most electronegative bacteria were *E. coli* and the least electronegative were *P. aeruginosa.* Baker's results indicated that more cells attached to the rough surface compared to the smooth surface. *S. aureus* attached the least to the hydrophilic rough glass surface which agrees with the theory above that hydrophobic species prefers hydrophobic surfaces. Another result of note was that the cell size increased upon attachment [43]. In addition, using *P. issachenkonii* bacteria, Baker proved that increased surface roughness increases cell attachment [44]. In summary, there are many factors that can affect the adhesion of bacteria to a surface.

1.3 Poly(dimethylsiloxane)

Polydimethylsiloxane, PDMS, is a silicone elastomer consisting of repeating units of $[(CH_3)_2SiO]_n$. PDMS has been used for many applications including microfluidics, lithography, prostheses, artificial organs, catheters, contact lenses, drug delivery systems, membranes, electrical insulators, water repellents, adhesives, and protective coatings [59-62]. It can be used for such a variety of applications because of its properties which include low density, hydrophobic surface properties that can be modified, low surface conductivity, low bulk conductivity, resistance to fractures over a wide range of temperatures, optical clarity, high gas permeability, and general inertness [59-62]. One

of the most used commercially available forms of PDMS is Sylgard-184 which is produced by Dow Corning. It is a kit including a base and curing agent. The base consists of siloxane oligomers with vinyl terminal groups and a platinum-based catalyst. The curing agent also contains siloxane oligomers with vinyl terminal groups as well as siloxane oligomers that are cross linked with three silicon-hydride bonds. The polymer cures due to the reaction of the cross-linked oligomers' Si-H bond over the double bonds contained in the vinyl terminated oligomers. This reaction, hydrosilation of the double bonds, forms -Si-CH_2-CH_2-Si- bonds which is shown in figure 1.6. Since there are multiple areas for the hydrosilation reaction to occur, three-dimensional cross-linking is possible [59].

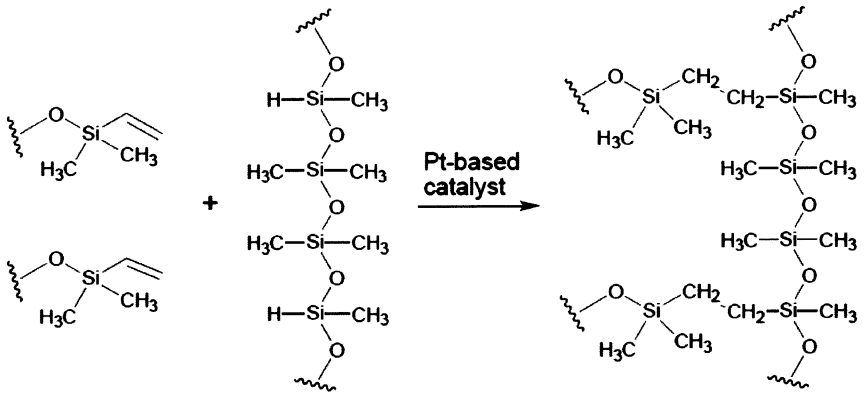

Figure 1.6 Cross-linking reaction of PDMS [59].

The useful surface properties of polydimethylsiloxane are due to the structure of this elastomer which include high strength and partial ionic character of the siloxane bond, backbone flexibility, and a low intermolecular force between the methyl groups [61]. The flexibility of the PDMS backbone is known to be one of the most flexible chain molecules meaning that the chain is capable of rotating around its bonds in the backbone. The flexibility is due to the long silicon-oxygen bonds (1.64 Å), the oxygen atoms being capable of multi-valency and having no large side groups, and the Si-O-Si bond angle being 143° compared to a regular tetrahedral angle of 110°. Since it has such high flexibility, PDMS has a very low glass transition temperature, -125°C, and a low melting temperature of -40°C [60, 61]. The low glass transition temperature occurs because of the segmental mobility and high free volume, and the low melting temperature is caused by the low enthalpy of fusion per mole of main chain bonds (2.75 kJ/mol) [62]. Another important property of PDMS is its high gas permeability which is used for soft contact lenses [60, 62]. PDMS is known to be water repellent meaning it has a hydrophobic surface chemistry; however, this characteristic can be modified [63].

Since polydimethylsiloxane is widely used in research, there have been many methods developed to modify the surface chemistry. The main methods to modify the surface include plasma treatment, UV irradiation, layer-by-layer (LBL) deposition, and silanization [66]. Plasma treatment involves a gas like oxygen, nitrogen, and argon that is partially ionized with electrons and ions forming radicals that react with the surface creating functional groups on the substrate surface [66, 68]. One of the first research groups to look at plasma treatment to modify polymer surfaces for adhesive bonding was J. R. Hall and colleagues [69]. Hall plasma treated PDMS elastomers using ammonia

plasma, but their results showed no NH_2 bonds [64]. Afterwards, Hollahan and Carlson determined the mechanism of changing the surface chemistry when using plasma treatments. They demonstrated that hydroxyl groups ($SiCH_2OH$) were formed on the PDMS surface when exposed to oxygen plasma [70]. M. J. Owen and P. J. Smith tested plasma treatment on PDMS using argon, helium, oxygen, and nitrogen gases. These tests yielded an increase in oxygen, decrease in carbon, and a stable amount of silicon compared to the control which was not plasma treated. The amount of carbon decreases and oxygen increases as the amount of time the polymer is plasma treated. When comparing plasma treatment using all four gases, there is a similar result with all gases except for nitrogen gas which shows nitrogen present [64]. In 2009, Moon and Vaziri used a multi-step plasma treatment to modify the PDMS surface but created tiered patterns. These researchers prestretched PDMS pieces in two different (biaxial) directions, exposed it to oxygen plasma treatment, and then released the stretching creating wrinkles on the surface. It was determined that the wrinkles can be modified based on the speed of stretch release. The creation of wrinkles on modified PDMS creates micron and submicron sized surface structural features [65].

Another method of modifying the PDMS surface is UV treatment which accomplishes the same result as plasma treatment. UV irradiation is slower to create the modified surface compared to plasma treatment; however, the modification is much deeper (10 μm) without causing cracking of the surface [66, 71, 72]. The UV treatment oxidizes the surface where the molecules of the polymer are excited/dissociated because it absorbs the short-wavelength UV radiation. UV treatment is usually done in the presence of nitrogen. When oxygen is present during UV irradiation, it is considered

UV/Ozone (UVO) treatment because molecular oxygen is broken down to atomic oxygen while ozone is constantly formed and destroyed due to absorption at 254 nm or 184 nm [71]. Efimenko, Wallace, and Genzer modified Sylgard-184 PDMS using UV and UV/Ozone treatment [71]. They exposed PDMS to UV radiation in the presence of just nitrogen or just oxygen. It was determined that for UVO treatment, as the irradiation time increased, the hydrophobic surface becomes more hydrophilic which coincides with an increase in surface energy. The UV treatment also showed an increase in hydrophilicity, but not as rapidly as UVO treatment. By using ATR-FTIR measurements, they concluded there was some chain scission in the PDMS surface, decrease in $-CH_3$ signal, and increase in –OH signal as UVO treatment time increased proving an oxidation of the surface creating hydrophilic species. For UV treatment, the same results were seen except no hydroxyl signal was observed. Lastly, the UV treatment was determined to create surface radicals creating different networks and surface end groups, whereas UVO creates a significant amount of hydrophilic groups [71]. Another example of UV modification is from the Graubner, Jordan, and Nuyken research group which used 172 nm irradiation on PDMS [63]. The irradiation was done by vacuum ultra-violet light using a Xe^2-excimer lamp. The results showed a linear decrease in contact angles using water and diiodomethane and an increase in surface free energy. They determined there were silanol groups on the surface based on contact angle measurements, X-ray photoelectron spectroscopy, and infrared spectroscopy [63]. Mirley and Koberstein used Langmuir-Bloggett layers to form ultrathin films of SiO_x on PDMS [67]. A carboxylic acid terminated PDMS was modified with an Langmuir-Bloggett film using wet

chemistry and compression of the polymer which was then exposed to UVO irradiation at 185 and 254 nm creating a hydrophilic surface [67].

Layer-by-layer (LBL) deposition is a wet-chemical technique to modify the surface of a substrate creating a polyelectrolyte multilayer on the surface. The method occurs by interspersing polyanions and polycations [66, 73]. The advantages include simple, fast, and thickness control; however, the disadvantages involve the multilayer structure, functionality, and stability which depend on ionic strength, ionic concentration, solvent, temperature, and pH [66]. An example of LBL deposition is from Qui and colleagues who alternated poly(diallyldimethylammonium chloride) and poly(sodium 4-styr-enesulfonate) to modify a PDMS surface [74]. The purpose of this modification was to produce a surface with reduced amount of non-specific adsorption [74]. The purpose of LBL deposition is to create a surface that is convenient for the research being done.

Silanization occurs where surface hydroxyl groups react with alkoxysilanes creating Si-O-Si bonds to the substrate. The terminal groups of the alkoxysilanes can be varied to include amines, thiols, or carboxyls [66, 75, 76]. Sui and coworkers oxidized a PDMS surface using H_2O, H_2O_2, and HCl creating silanol groups which were then reacted with alkoxysilanes [75]. Slentz, Penner, Lugowska, and Regnier used 1 M NaOH to modify the surface of PDMS [76]. They soaked the PDMS in NaOH for one day creating silanol groups on the surface [76].

Even though the surface of PDMS can be modified from a hydrophobic surface to a hydrophilic surface using plasma and UV/UVO treatments, there is hydrophobic recovery seen over time. According to Morra et al. hydrophobic recovery is due to

silanol condensation seen in figure 1.7 which causes a reduction in the number of polar groups on the modified PDMS surface and increased amount of cross linking [77].

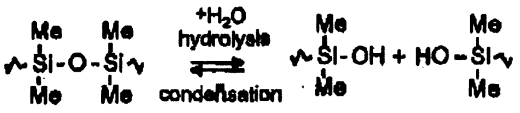

Figure 1.7 The silanol condensation reaction mechanism that causes hydrophobic recovery [62,77].

There is also a movement of bulk chains to the modified surface as well as rotation of polar groups into the bulk causing the reduction in hydrophilicity [74]. The polar groups are able to rotate back into bulk because of the flexibility of native and modified PDMS, and it is caused by the need for minimization of solid interfacial tension [62, 78]. The most common method of hydrophobic recovery is the movement of bulk chains to the surface of the modified PDMS, and it was first proposed by Lee and Homan [62, 79]. A schematic showing formation of cracks and movement of bulk chains is seen in figure 1.8. It has been shown that when cracks occur on the surface of the hydrophilic PDMS, there is an increased rate of hydrophobic recovery [81]. The cracking of the hydrophilic surface is caused by PDMS distortion above a very low amount of strain, and it can also be caused unexpectedly [62].

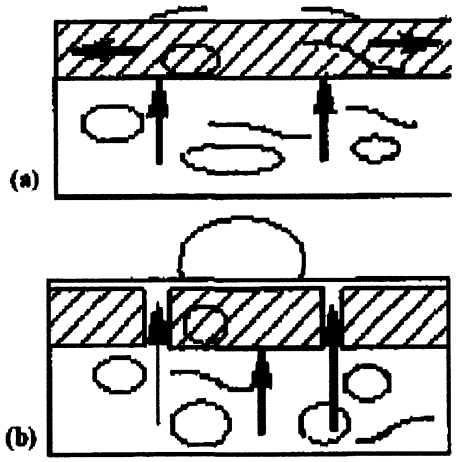

Figure 1.8 The movement of bulk chains to the surface after formation of cracks have occurred rendering the PDMS surface hydrophobic [62].

Once the crack has occurred, the low molecular mass molecules located in the bulk move from the cracked area up the hydrophilic surface by pore diffusion [62]. The surface of PDMS has many properties that allow it to be useful as a native surface or a modified surface, and as long as the hydrophobic recovery is known, it can be avoided to some extent.

1.4 Characterization of 254 nm Irradiated Sylgard-184 Polydimethylsiloxane

Waddell et al. has previously developed a quick and simple method to create carboxylic acids on the surface of PDMS by irradiating at a mercury line wavelength of 254 nm. The advantages of this process include it being a one-step process, accessible to most facilities, no specialized skills needed, inexpensive, and environmentally friendly. The modified surface was characterized using contact angle measurements, infrared spectroscopy, atomic force microscopy (AFM), and scanning electron microscopy (SEM). The contact angle measurements showed a decrease in the contact angle as the

amount of irradiation time increased indicating an increase in hydrophilicity of the surface. However, the contact angle decreased until a plateau was reached at two hours which can be seen in figure 1.9 [82].

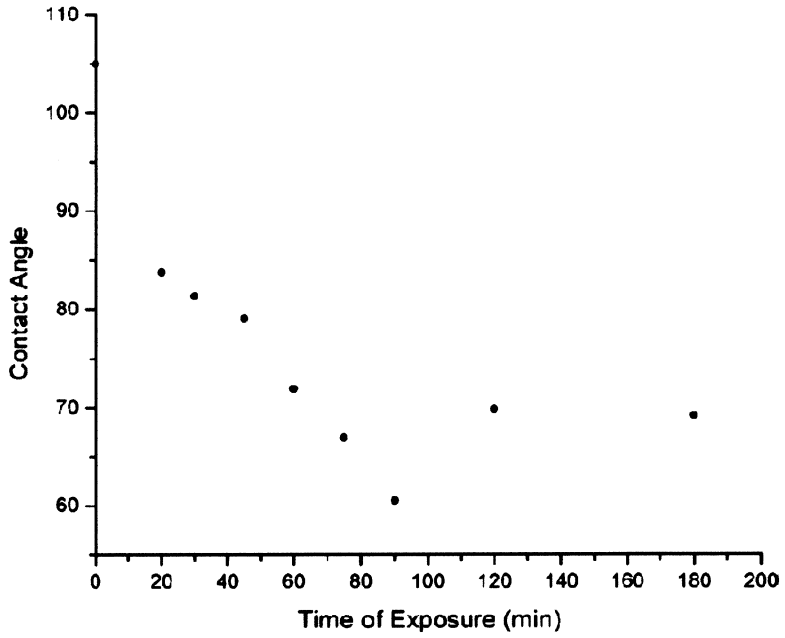

Figure 1.9 Contact angle measurements with varying amount of irradiation time at 254 nm [82].

The plateau of contact angle measurements coincides with the formation of an inorganic, glassy layer that forms on the surface with increased irradiation time causing a breakdown of the PDMS backbone. Infrared spectroscopy was completed on native and irradiated PDMS surfaces. As the irradiation time increased, an increase in hydroxyl groups on the surface and a breakdown of the PDMS backbone was observed [82].

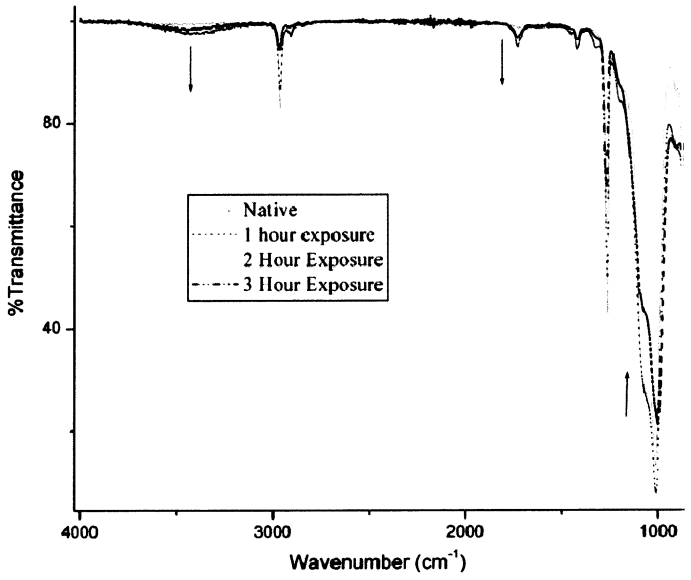

Figure 1.10 ATR-FTIR data of native PDMS and PDMS irradiated at 254 nm for 1, 2, and 3 hours [82].

The ATR-FTIR data above in figure 1.10 shows an OH stretch at 3400 cm^{-1} that increased in intensity as the amount of irradiation time increased as well as a band at 1725 cm^{-1} indicating the presence of carboxylic acids on the PDMS surface. The breakdown of the PDMS backbone can also be seen on the ATR-FTIR data which are seen in the symmetric and antisymmetric methyl group stretch at 2966 cm^{-1} and 2905 cm^{-1} respectively, and the reduction in the asymmetric stretch of the Si-O-Si bond at 1089 cm^{-1} and 998 cm^{-1}. Lastly, the atomic force and electron microscopy showed increased hardness and roughness of the surface as well as formation of cracks. AFM determined the surface roughness of the native PDMS in ambient conditions was ~6.2 ± 2 nm and in PBS was ~12 ± 4 nm. After irradiation for two hours the surface roughness in PBS increased to ~28 ± 9 nm in addition to pits the diameter of 2 – 10 nm [82].

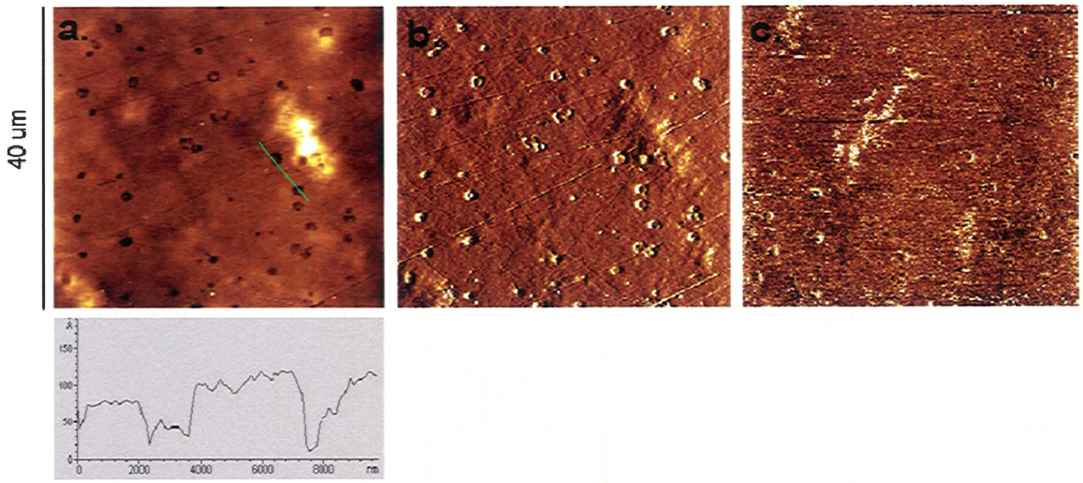

Figure 1.11 AFM images from irradiated PDMS indicating increased surface roughness as irradiation time increased [82].

The increased surface roughness is due to the increased irradiation time. The AFM images in figure 1.11 show that the inorganic siloxane glassy layer is extensive, but also correlates with the increase in irradiation time, surface stiffness, and the plateau seen in the contact angle measurements. The SEM images in figure 1.12 showed cracks and crazing on the modified PDMS surface which were found to correspond with the plateau seen in the contact angle data [82].

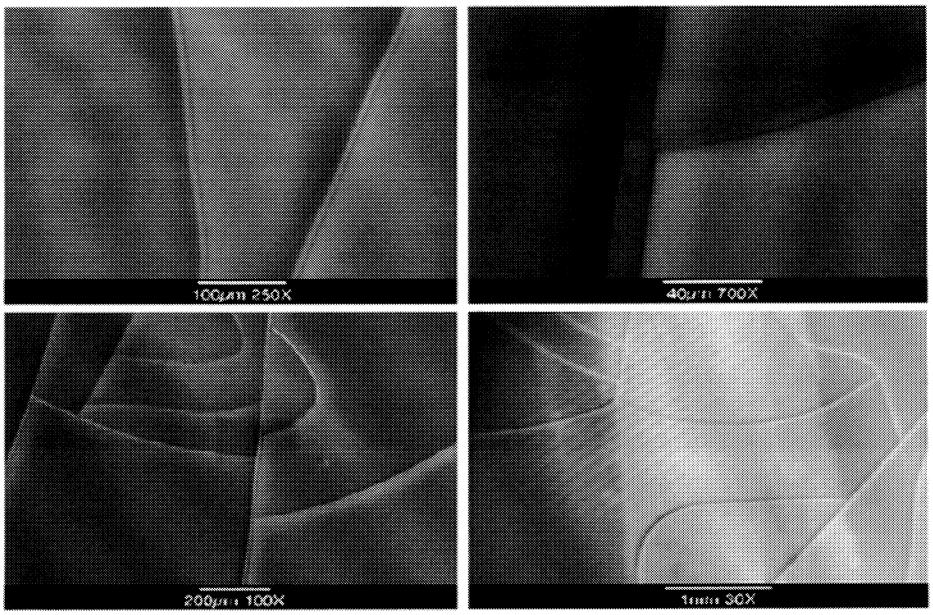

Figure 1.12 SEM images of the crack formation on irradiated PDMS [82].

The cracks had a width of 10 μm and a depth of 2 μm [82]. The formation of pits on the surface comes before the crack formations which is a result of surface relaxation [83, 84].

1.5 Characterization of PDMS Irradiated at 254 nm Using a Mercury Lamp

The mechanism of carboxylic acid formation by the irradiation at 254 nm was proposed by Hillborg and Gedde. The reaction scheme can be seen in figure 1.13.

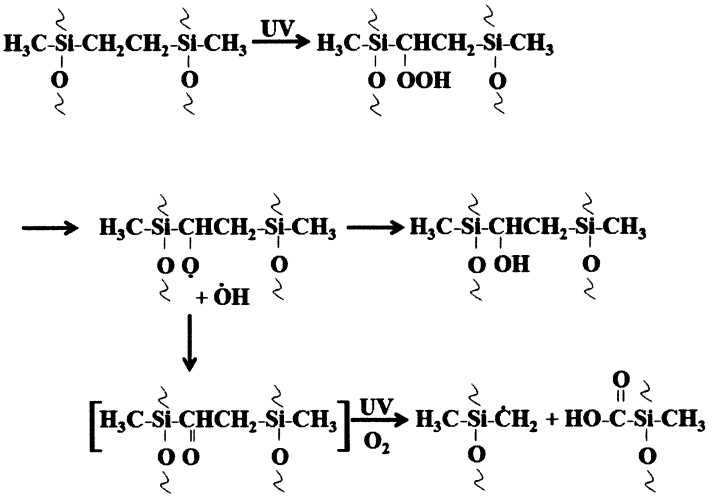

Figure 1.13 Proposed mechanism of carboxylic acid formation with irradiation at 254 nm [62].

Contact angle measurements were performed on native PDMS and PDMS that had been irradiated at varying amounts of time, and the results can be seen in figure 1.14. The native PDMS had a contact angle of 105°, and as the irradiation time increased the contact angle decreased until an irradiation time of 75 minutes which had the lowest contact angle observed, 54°. After the 75 minutes of irradiation, cracks were observed causing a slight increase in the contact angle due to migration of bulk chains to the surface [85].

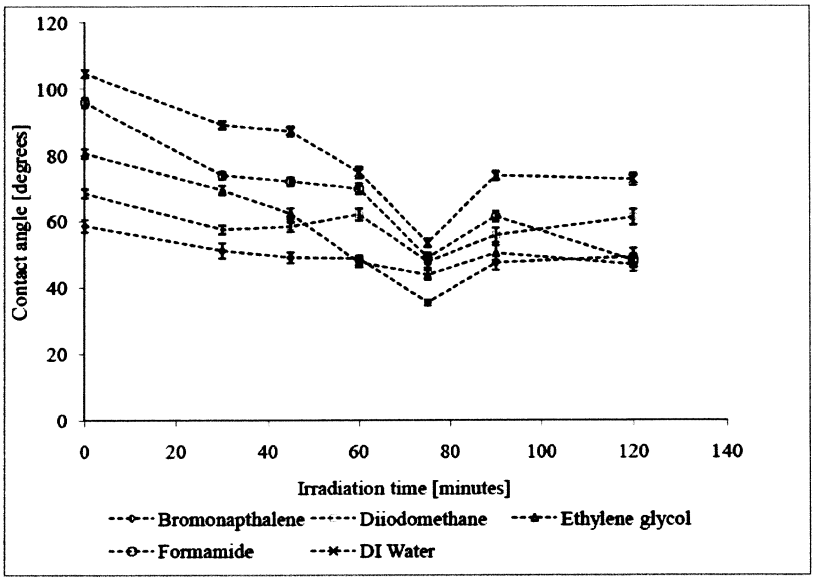

Figure 1.14 The contact angle measurements with different liquids at varying amount of irradiation time [85].

The surface energy of the native and irradiated PDMS was analyzed, and the results are depicted in figure 1.15. It was determined that as the irradiation time increased to 75 minutes, the surface energy increased from 21.9 mN/m for native to 47.5 mN/m for 75 minutes of irradiation. It was also seen that as the surface energy increased, the polar component increased while the dispersive component decreased. This was seen until 75 minutes of irradiation because formation of cracks occurred affecting the surface polarity. After 90 minutes of irradiation, there was no change in surface energy [85].

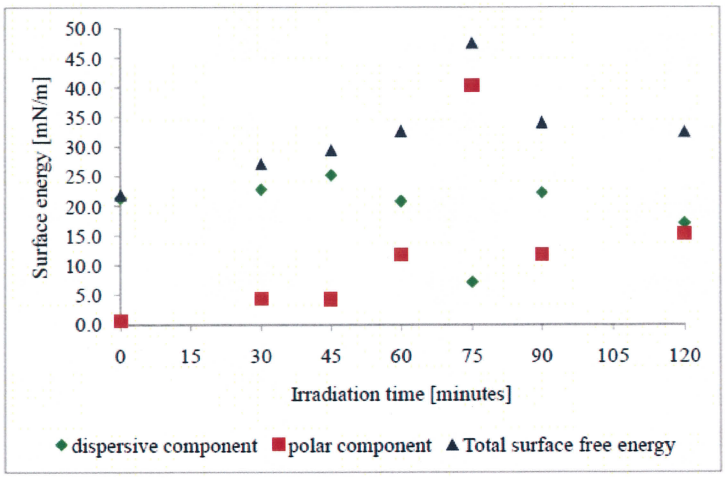

Figure 1.15 The surface energy of PDMS surfaces irradiated at various times [85].

Infrared spectroscopy showed peaks at 1725 cm^{-1}, a carbonyl stretch, and at 3300 cm^{-1}, a hydroxyl band for irradiated PDMS which was not seen for native PDMS. Together, these two bands indicated the presence of carboxylic acids on the surface of the irradiated PDMS. As the irradiation time increased up to 75 minutes, the carbonyl stretch peak increased in intensity, and afterwards, there was a decrease in intensity which is seen in figure 1.16. This observation indicated that as the irradiation time increased up to 75 minutes, the amount of carboxylic acids present on the surface increased as well until the degradation of the PDMS backbone was seen with the decay of band intensity. This result correlated the contact angle measurements and the surface energy values because as the contact angle decreased, there was an increase in surface energy, and an increase in the amount of carboxylic acids on the surface [85].

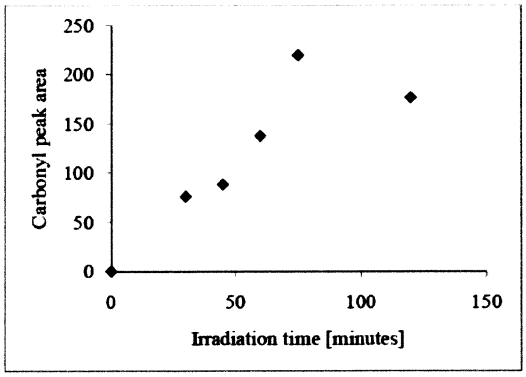

Figure 1.16 The intensity of the carbonyl peak seen for PDMS irradiated at various times [85].

Since an increase in irradiation time up to 75 minutes showed an increase in the carbonyl peak of the IR spectra, the amount of carboxylic acids present on the irradiated PDMS surface was determined using methylene blue dye staining. The methylene blue dye will only attach to the carboxylic acids present on the irradiated PDMS surface, so the higher absorbance value indicates a higher amount of carboxylic acids present. It was determined that the most carboxylic acids present occurred at 75 minutes of irradiation. In general, the number of carboxylic acids increased until 75 minutes and afterwards greatly decreased which can be seen in the graph of figure 1.17. The decrease in amount of carboxylic acids was caused by the formation of a glassy layer on the surface due to the degradation of the PDMS backbone. The concentration of carboxylic acids present on the surface was determined from the surface area of PDMS used and the concentration obtained from the methylene blue experiment converted to the number of carboxylic acid molecules per unit area of PDMS.

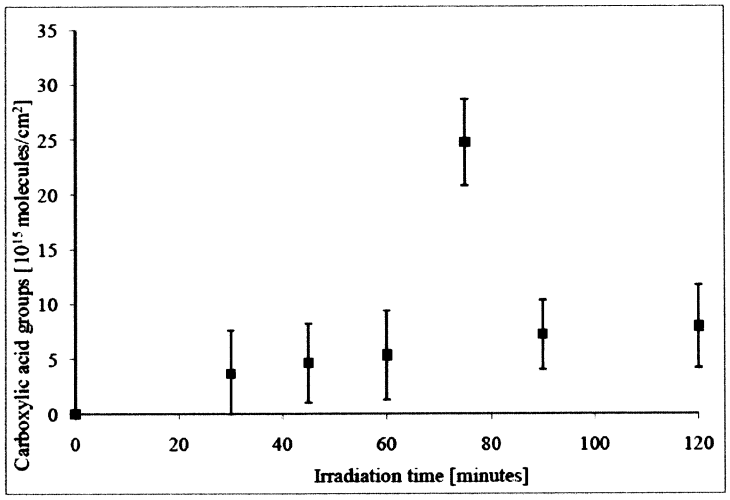

Figure 1.17 The concentration of carboxylic acids present on PDMS surfaces irradiated at various times. This experiment is reproducible, and it was repeated six times [85].

The maximum concentration of carboxylic acids was determined to be 2.5 x 10^{16} molecules/cm^2 which occurred at 75 minutes of irradiation [85].

The stability of the carboxylic acids on the PDMS surface was studied to determine the best way for storage because hydrophobicity recovery occurs. Multiple storage methods were analyzed including air, water, ethanol, PBS, pH 10 sodium hydroxide solution, and a 50 % acetic acid solution. When a PDMS coupon that was irradiated for 45 minutes was stored in water, the hydrophobicity started occurring one day later and after 7 days completely recovered. The other methods were also tested using a 45 minute irradiated piece of PDMS. When stored in air, water, PBS, ethanol, and a pH 10 sodium hydroxide solution, the hydrophobicity recovery occurred because when analyzed using infrared spectroscopy, there was a decrease in the intensity of the carbonyl stretch band at 1725 cm^{-1}. The only method that kept the irradiated PDMS unchanged was the 50% acetic acid solution. This was verified by infrared spectroscopy

and by contact angle measurements which both showed stable results [85]. The contact angle results can be seen in figure 1.18

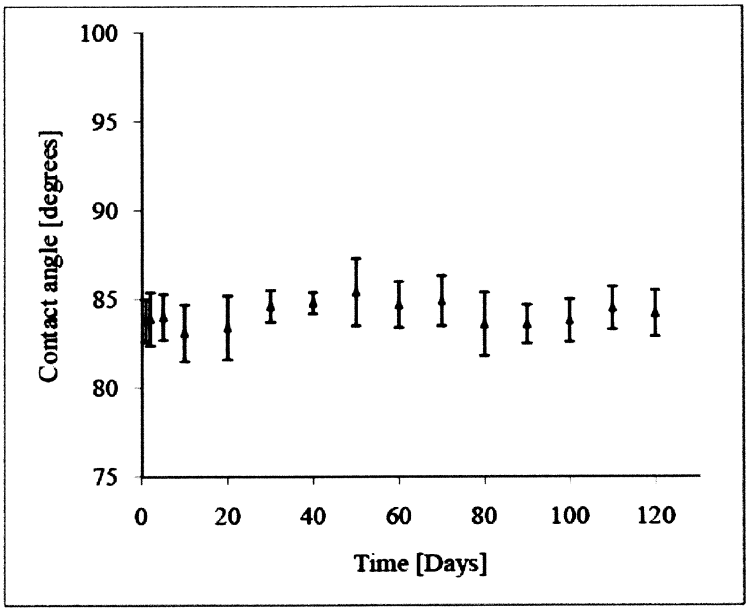

Figure 1.18 The contact angle for PDMS irradiated for 45 minutes and being stored in 50 % acetic acid solution for an increasing amount of days [85].

The contact angle measurements were done over four months, and a stable contact angle of 84° was maintained verifying that the PDMS surface stayed hydrophilic [85].

1.6 Objective

The formation and characterization of carboxylic acids on PDMS irradiated at 254 nm using a mercury lamp has been well documented. The purpose of this research is to attach *E. coli* to the irradiated PDMS to understand the basics of cell attachment. It has been shown that *E. coli* and other bacteria can attach to different modified polymer

surfaces with SAMs being the most popular mechanism to modify surfaces for cell attachment. The aim of this project is to attach the *E. coli* to the carboxylic acids present on the irradiated PDMS surface and investigate the optimal conditions for attachment to ultimately pattern the cells on PDMS.

1.7 Thesis Outline

First, a literature review is provided to show how other researchers have performed cell attachment and modification of a PDMS surface. An explanation of previous research on the modified PDMS surface has then been presented including the method of carboxylic acid formation followed by characterization of the surface using multiple techniques. This is followed by a description of the instrumentation used for this research, experimental techniques, results and discussion, and future works.

CHAPTER 2

INSTRUMENTATION

2.1 Confocal Microscopy

The confocal microscope was invented by Marvin Minsky in 1955 while a Junior Fellow at Harvard University. For his doctoral thesis, he studied many aspects of the nervous system but on connectivity in particular. At that time only the cell shape of a neuron was known from staining by the Golgi treatment. However, if a complete slice of a brain which contains many neurons was stained only a blur would be seen under the microscope. Due to limitations of current microscopes, he constructed the first confocal microscope. He first began by wanting to remove unwanted scattered light from being collected in the condenser. He realized that a perfect microscope would illuminate a single point on the specimen and the light scattered or absorbed from that single point would be measured/collected. To make this possible, he decided that if a second microscope replaced the condenser, a pinhole aperture could be imaged onto a single point of the specimen which reduced the light in the specimen but did so without affecting focal brightness. Then to remove the light scattered by points near the focal point, a second pinhole aperture was placed in the image just after the exit side of the

objective lens. The final setup was a pinhole and objective leans on both sides of the specimen or one side could have half-silvered mirrors separating entering and exiting rays which can be seen in figure 2.1 [86].

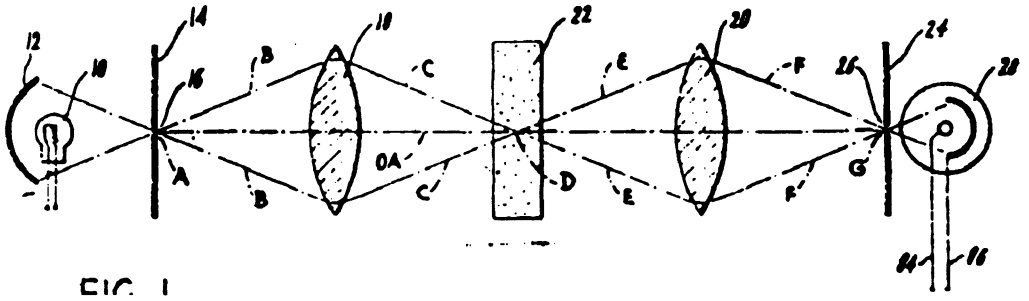

Figure 2.1 The optical setup of Minsky's confocal microscope [86].

The light source used was a zirconium arc because it was more dependable than a carbon arc. Since only a single point of the specimen was illuminated, the microscope had to scan the specimen by moving the optics or moving the specimen. Minsky chose to move the specimen, because if the optics were moved, there would be the problem of continuously aligning two small moving apertures. The specimen was placed onto a platform that moved vertically in a sinusoidal waveform and horizontally in a sawtooth waveform. The electric signals controlling the platform also scanned the specimen image onto a long persistence radar scope [86]. At the time this microscope was invented, the possible applications were not used by scientists. During the 70's and 80's fluorescence microscopes became very popular because fluorescence labeled antibodies and fluorescent dyes became widely used. Fluorescent labeled antibodies were able to

determine the cytoskeleton of cells, and fluorescent dyes revealed intracellular pathways. The fluorescent microscope became limited in that the minute details of the thick specimen could not be seen because of a uniform glow due to out-of-focus points. In the late 80's, J. G. White looked into Minsky's confocal microscope. It was determined that studying fluorescence with a confocal microscope that moved the specimen was very time consuming. The correct focus and the correct region of the specimen were difficult to find and sometimes the image came out blank. White developed a prototype that moved the beam and scanned the specimen by using a "flying spot" invented by Young and Roberts in 1952 [87, 88]. The "flying spot" required that the beam fill the entire back aperture at all times, the beam must rotate around a point in the aperture plane, and produce a translation of the focused spot in the plane of focus [87, 88]. The prototype contained a single reflector in the back aperture that could tilt in two orthogonal directions which occurred by using a slow oscillating mirror and a fast polygonal mirror allowing for a high scanning rate [87]. A schematic of White's prototype can be seen in figure 2.2.

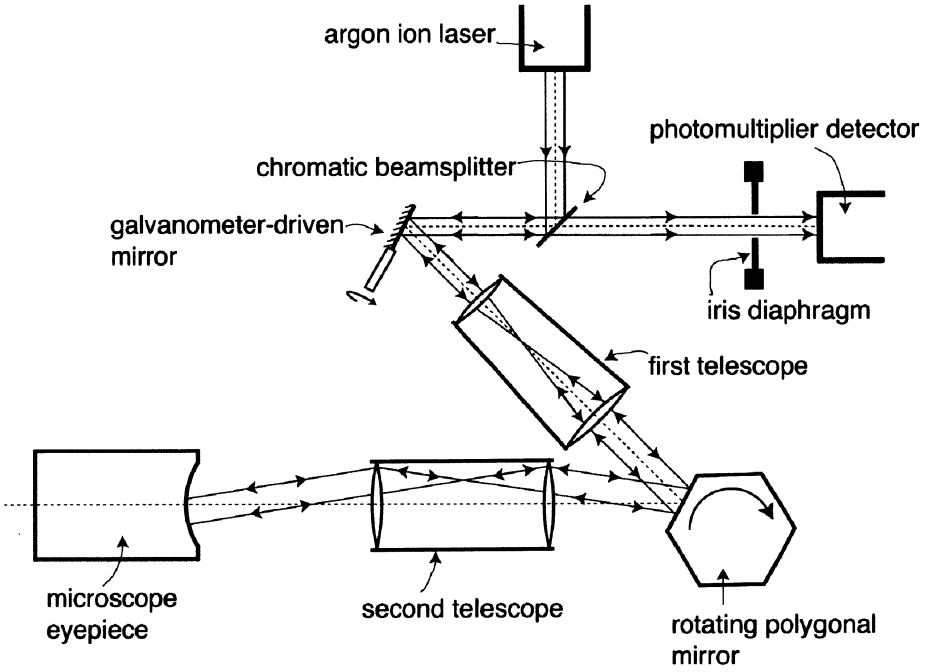

Figure 2.2 Schematic of White's confocal microscope prototype [87].

One of White's research students, Richard Drubin, developed software to run with the confocal microscope called scanning optical microscope (SOM). This prototype was developed commercially by Bio-Rad and called MRC 500 [87].

2.1.1 Basic Configuration

Confocal microscopy has become increasingly popular in recent years because of its high quality images and the increasing amount of applications in biology and other disciplines. It has the ability to control depth of field, remove background information from focal plane, and create optical sectioning of thick specimens all due to the elimination of out-of-focus light by spatial filtering techniques. The most basic confocal microscope is a laser scanning confocal microscope. In general, a laser system emits coherent light that passes thought a pinhole aperture. The pinhole aperture is in a

conjugate plane with the point on the specimen being scanned and another pinhole aperture in front of a photomultiplier tube or detector. The apertures have to be in a conjugate plane to allow for correct illumination of the specimen. When the laser beam scans the specimen, it does so in a raster pattern; however, when the fluorescence is emitted it stays steady at the pinhole aperture only changing with intensity over time. When the laser scans the specimen at a defined focal point, other points on the specimen fluoresce as well which are above and below the focal plan (out-of-focus). Most of the out-of-focus fluorescence is not part of the final image of the specimen since it does not go through the detector pinhole aperture. By refocusing the objective, a different plane of the specimen can be viewed. The excitation and emission points would change to the needed plane which then is the conjugate plane of the two pinhole apertures. At the end, a photomultiplier converts the fluorescence to an analog signal with continuous voltage varying with the corresponding intensity which is then converted to pixel by an analog-to-digital converter. Finally, the image is displayed onto a computer [89].

2.1.1.1 Light Sources

Lasers are used in confocal microscopy because of their properties including a high degree of monochromaticity, small divergence angle, high brightness, high degree of spatial and temporal coherence, plane polarized emission, and a Gaussian beam profile. There are many different laser systems in use and vary in physical size, operation, and mechanical properties due to design, emission wavelength, operation difficulty, costs to maintain, and reliability. The laser power should be between 10 – 100 μW or less than 1 mW of continuous wave for best results. In the confocal microscope used at UAH, solid-state lasers are used [90].

These lasers are power-efficient, versatile, and easy to operate as a continuous wave, as a pulsed direct light source, or as a pump source for other lasers [90].

2.1.1.2 Objectives

The objective lens is a very important component in microscopy, in particular confocal microscopy. The objective lens determines the information sent to the detector for the image of a specimen. It has the ability to resolve detail and determine contrast, depth, and diameter of field needed to obtain the correct information of the image [90]. The information obtained by the objective lens is sent to a detector. There are a wide variety of detectors including simple point detectors like photomultiplier tubes and array detectors. The purpose of detectors is to give the highest quantum efficiency, the lowest background level, and the highest signal-to-noise ratio [90].

2.1.2 Resolution and Contrast

An important aspect of confocal microscopy is resolution and contrast which have an interdependent relationship. Resolution is defined as the smallest amount of distance that two objects can be distinguished or allows a certain quantity of contrast between the two objects. For a perfect optical system, resolution depends on numerical aperture and the light wavelength, and contrast depends on the amount of collected photons, signal range, optical aberrations, and amount of pixels per unit area. For resolution and contrast, the amplitude spread function and the intensity point spread function have to be discussed for airy disk and lateral resolution first. The amplitude spread function allows the analysis of the amplitude fluctuations caused by the electromagnetic field in the image plane when imaging the specimen. The fluctuations are due to the optical system reacting to the specimen. The intensity point spread function is defined as the systems

response in real space to field amplitude fluctuations which can be seen as the point source image recorded. Resolution of an image depends greatly on the image plane intensity point spread function described by airy disk and axial intensity point spread function. The image plane intensity PSF can be described by the airy disk because the microscope lenses are symmetrical and the x and y components of the airy disks are equivalent allowing this measurement to be the intensity as a function of optical axis distance. When a fluorescent emission occurs, it does so in all directions; however, only the focused light will enter the aperture in front of the detector. When this occurs, airy disks form concentric rings around the focused point on the specimen, and the rings are sequentially decreasing maximum and minimum intensities creating an airy pattern. When considering an image's resolution, the image is considered the sum of two airy disks because resolution is defined as the distance two objects can be distinguished and each object creates its own airy disk. In the figure below, intensity point spread functions and airy disk intensities can be seen with varying distance between two objects being resolved [91]. A visual representation explaining resolution and contrast can be seen in figure 2.3.

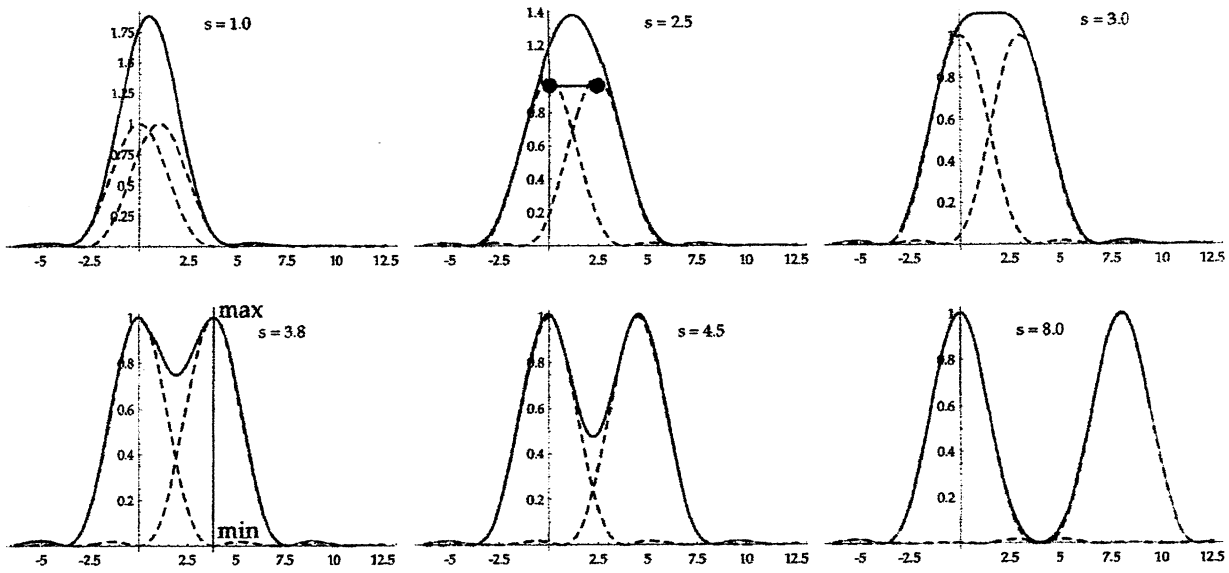

Figure 2.3 Comparison of airy disks intensity (dotted lines) and intensity point spread function (dark lines) [91].

As can be seen from the figure above, when there is enough distance between the two objects, their corresponding intensity peaks are also separated in the intensity point spread function. As the distance decreases the two intensity peaks begin to overlap causing the two objects to appear as one brighter object. The better resolution, the separation of the intensity peaks and airy disks peaks is greater. This is where the concept of resolution being best at full width half maximum of the intensity point spread function for the microscope comes from. The contrast in relation to intensity point spread function is defined as the maximum and minimum intensity difference between the two objects intensity peaks for the airy disks. For best contrast, the airy disks peaks are completely resolved with the intensity at zero at the combined intensity distribution. As the peaks overlap where the intensity dip decreases almost creating one peak, the contrast greatly diminishes. The contrast-cut off distance occurs when the two peaks

cannot be distinguished, and the contrast is zero. The axial point spread function works in the same way as the lateral point spread function when analyzing resolution and contrast [91].

2.1.3 Signal-to-Noise

The next aspect of confocal microscope is the signal-to-noise ratio. The signal is determined by the amount of photons the detector collects from the specimen, but the signal level is proportional to the amount of photons collected. The variation in the amount of photons collected with repeated measurements is considered the noise of the instrument. The noise affects the quantification of intensity which then affects the resolution and contrast. When using the confocal microscope to view a specimen without fluorescence (reflection contrast) the sources of noise are due to the electronics of the instrument and the variation in illumination. For fluorescence imaging, the Poisson noise is the main source of noise which is based on the statistical variation in the amount of photons collected by the detector. Another type of noise is shot or photon noise which occurs during fluorescence microscopy where signal is low, limiting the amount of photons that can be detected which also increases signal variation due to the difference in arrival times of the photons. The basis of the shot noise is the particle nature of light and the photon's electrical characteristics. The signal-to-noise ratio affects the quality of the image. The higher the signal-to-noise ratio causes a better image to be seen. The image quality is affected because this ratio is related to contrast in the fact that the fluctuation in intensity determination decreases the contrast, and the noise reduces the resolution. To increase the signal-to-noise ratio, the aperture pinhole can be increased to a certain limit where at that point it begins to decreases due to increased background signal over

powering it. To get the best ratio, the aperture pinhole has an optimum size depending on the instrument [91].

2.1.4 Advantages and Disadvantages

Lastly, the advantages and disadvantages of the confocal microscope will be discussed. The advantages are the ability to optically section thick specimens up to 50 μm, and to form composite and multi-dimensional images and videos from z-series image stacks. The disadvantages include limited amount of laser lines, damage to cells and tissues, and high cost. The main advantage of a confocal microscope is the ability to optically section thick specimens. The sections are formed by synchronizing incremental changes in fine focus with continuous image collection at each step. Compared to widefield microscopy, confocal microscopy has better contrast and definition due to reduced background fluorescence and increased signal-to-noise ratio. Artifacts do not occur unlike when physically sectioning and staining specimens. The optical sectioning can be performed on living or fixed specimens with equal clarity and varied conditions. The optical sectioning can be done in the normal x-y plane as well as x-z and y-z planes or vertical sections. One of the disadvantages is the limited amount of laser lines which are the laser excitation wavelengths. The laser lines are over very narrow wavelength bands, and ones in the ultraviolet regions are expensive. However, the widefield microscopes are capable of producing wavelengths in the ultraviolet, visible, and near-infrared regions using mercury or xenon arc-discharge lamps. Another disadvantage is the damage the laser irradiation causes on the living specimens. Lastly, the cost of buying and operating a confocal microscope is expensive compared to widefield

microscopes; however, if the confocal microscope is shared by multiple labs, the cost becomes more bearable [89].

2.1.5 Conclusion

The confocal microscope is an instrument that will be significantly used for a wide application of research and will continuously be improved on. In this research, the expectations of the confocal microscope include imaging the chemically attached *Escherichia coli* on the modified polydimethylsiloxane (PDMS) at 10X and 63X using oil immersion. The microscope allows for the bacteria to be easily and clearly identified.

2.2 Contact Angle

Wettability is the ability of a liquid to spread across a flat solid surface, but can also define a liquid defusing into a porous solid or one liquid displacing another [92]. When a liquid drop is placed onto a surface, the shape it takes depends on the cohesive forces of the liquid and adhesive forces of the liquid and solid. The cohesive forces are the intermolecular forces between the liquid molecules. Also, a cohesive force on the outermost layer of molecules in the liquid drop is the surface tension of the liquid. The adhesive forces are the intermolecular forces interacting between the surface and liquid molecules. It has been determined that a liquid will easily wet a surface when it has a low surface tension because adhesive forces dominate. When the liquid has a high surface tension, the solid is not as wettable, and the drop will ball up compared to the lower surface tension liquid since cohesive forces dominate. Wettability can be quantitatively measured using contact angles. When the liquid is in contact with the surface, a contact angle is created with the cohesive and adhesive forces determining it. The low surface tension liquids usually give a contact angle of zero or close to zero

because the adhesive forces are stronger. High surface tension liquids create a definite contact angle because cohesive forces predominate over the adhesive forces [93]. Another term describing wettability is spreading and nonspreading. When the liquid does not easily spread on the surface, it is called nonspreading which has a contact angle that is not equal to zero. The liquid is considered spreading when the contact angle is equal to zero [94]. The varieties of drop shapes can be seen below in figure 2.4 where θ indicates the contact angle.

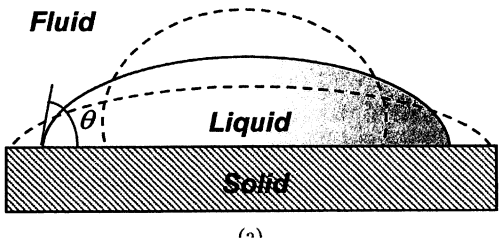

Figure 2.4 Different shapes a drop of liquid can take [95].

When wettability is discussed, sometimes hydrophilic and hydrophobic are commonly used, but these terms are in reference to water. Hydrophilic means the water easily spreads over the surface and hydrophobic surfaces causes the water to create a definite contact angle and does not easily spread or wet the surface.

2.2.1 Contact Angle Measurement Method

An ideal contact angle is one where the liquid drop and solid surface are in equilibrium. A Young contact angle is based on the Young equation and is normally

considered the ideal contact angle. It is dependent on the three-phase physio-chemical properties, but independent of gravity and the geometric shape of the system. An actual contact angle is where the liquid is in a local equilibrium with a rough or heterogeneous solid surface. An apparent contact angle is where the liquid is in macroscopic equilibrium with a rough or heterogeneous surface. An advancing contact angle is a liquid drop that is in equilibrium with the solid and has the highest apparent contact angle. A receding contact angle is in equilibrium with the solid surface and has the lowest apparent contact angle. The most stable contact angle is one where the apparent contact angle has the lowest Gibbs energy for that wetting system. A dynamic contact angle is measured where the liquid is in motion at a noticeable velocity [95].

Measurement of contact angles can be accomplished using different methods that have been developed. The methods include the captive bubble method, the tilting plate method, the Wilhelmy slide/plate technique, and the sessile drop technique. The two most common techniques are the sessile drop and Wilhelmy plate method [92, 96].

The sessile drop method is the most widely used method [98]. For this method, a drop is placed on a horizontal flat solid surface and is depicted in figure 2.5 [92].

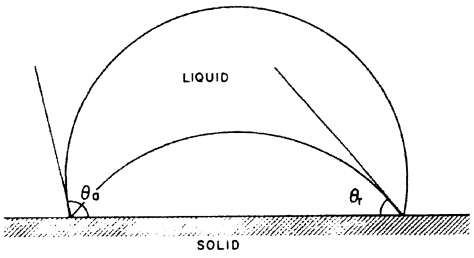

Figure 2.5 Sessile drop method of a liquid on a horizontal surface and the location of advancing and receding contact angles [92].

The cross section view of a drop is visualized in a telescope, and a goniometer in the eyepiece of the telescope is used to measure the contact angle directly [92]. In modern equipment, an image of the drop can be taken, and the contact angle determined using software. To increase accuracy a magnification up to 50X is ideal so that the liquid and solid interface can clearly be seen. To ensure the correct part of the drop is in focus, the reflection on the surface, the telescope should be tilted one to two degrees out of the horizontal position with the surface. The tangent to determine the contact angle is placed at the point where the liquid is in contact with the surface. A light source shining through a diffuser glass plate is used with this method to reduce any unwanted heating of the liquid and assist with the reflection of the drop. Receding and advancing angles can be determined using this technique as well. A micrometer syringe is used to slowly grow the sessile drop. The needle is not removed from the drop because it can allow vibrations to cause a lower contact angle than expected. The needle in the drop does not affect the contact angle unless it is larger than one-fifth the size of the drop causing distortion. To advance the drop, small amounts of liquid are added to the drop using the syringe [98]. The receding angle is found in the same way except that liquid is slowly removed from the drop [96]. When making measurements, several drops are measured, and angles on both sides are measured and averaged to allow for deviation of the surface chemistry. Some precautions to follow include measuring the angle immediately after adding liquid for an advancing angle and not letting the drop get smaller than 0.01 mL when measuring receding angles. The advantage of the sessile drop method includes ease and quickness [92].

2.2.2 Young's Equation and Other Mathematical Advancements

When most liquids are placed onto a flat solid surface, the liquid does not wet the surface, and instead creates a definite contact angle that can be used to determine other surface chemistry characteristics. In 1805, Young determined the relationship between a contact angle and the surface tension of solid-liquid, solid-vapor, and liquid-vapor interfaces which can be seen in equation (1) [99]. However, it was Dupre who actually published the equation which can be seen in equation (2) below [100].

$$\gamma_{SL} - \gamma_{SV}^{\circ} + \gamma_{LV}\cos\theta = 0 \tag{1}$$

$$w_{SLV} = \gamma_{LV}(1 + \cos\theta) \tag{2}$$

The above two equations are equivalent, but equation (2) uses the work of adhesion, w_{SLV} [97]. Gibbs further modified the equation and used thermodynamics to minimize the system free energy. By doing this, the surface tension of the solid-vapor and solid-liquid no longer had to be known independently since they are difficult to measure making only the surface tension of the liquid-solid necessary. The Gibbs equation is below in equation (3).

$$\cos\theta = (\pi_{s/l} - \pi_{s/v}) / \gamma_{lv} \tag{3}$$

$$\text{Where } \pi_{s/l} = \gamma_{s/o} - \gamma_{s/l} \text{ and } \pi_{s/v} = \gamma_{s/o} - \gamma_{s/v}$$

The term $\pi_{s/l}$ measures the liquid's ability to spread across the liquid, $\pi_{s/v}$ opposes the liquid spreading across the solid, and γ_{lv} determines if the liquid will ball up due to surface tension forces. These terms can be visualized as vectors of the three phases which can be seen in figure 2.6 [92].

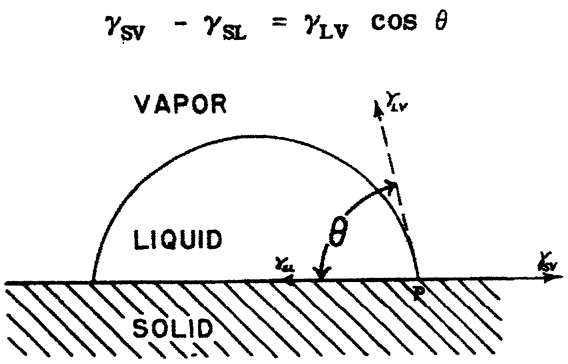

Figure 2.6 A sessile drop on a solid surface showing the location of the three interfaces: solid-liquid, solid-vapor, and liquid-vapor. Young's equation can be seen at the top [94].

Years later, Zisman and Fox determined a linear relationship between cos θ and γ_{LV}° for organic liquids. When a plot of cos θ vs. γ_{LV}° is created, the critical surface tension of the solid can be determined by extrapolating the line to cos θ = 1. The intercept of this linear line defines the critical surface tension of the solid. The line is linear for organic liquids but when liquids hydrogen bond with the solid surface, curvature in the line is seen. An example of a Zisman plot can be seen in figure 2.7 [94].

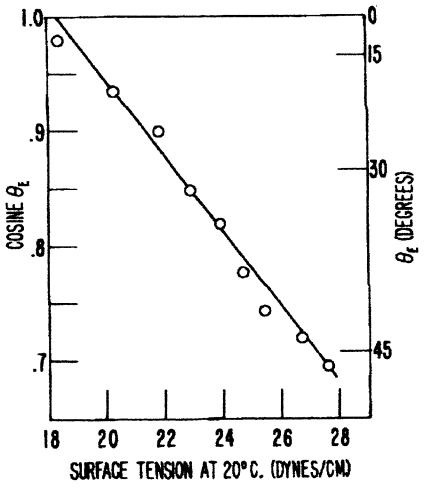

Figure 2.7 An example of a Zisman plot using polytetrafluoroethylene as the solid and n-alkanes as the test liquids [94].

For example, if multiple liquids were tested on a single type of polymer, contact angles could be determined by measuring multiple drops on the surface and averaging the contact angles. Once the contact angle for that liquid on the particular solid is determined, the cosine of the angle can be determined. The surface tension of the particular liquid can be looked up in reference tables. A Zisman plot can be created from the cos θ values versus the surface tensions of the liquids. Lastly, the linear line can be extrapolated to cos θ = 1 to find the critical surface tension of the solid. The Zisman plot and the Young's equation in particular require the surface to be homogenous and flat [94].

2.2.3 Hysteresis

As mentioned during the methods section, advancing and receding contact angles are determined in most instances. When the advancing and receding contact angles are

not identical, it is called hysteresis [97]. The advancing angle can occur by either adding liquid to increase the volume of the drop or allow the surface to cool below the dew point causing condensation to add liquid to the drop. The receding angle can occur by either removing liquid from the drop or by allowing the liquid to evaporate from the drop [101]. The advancing and receding angles can be seen in figure 2.8.

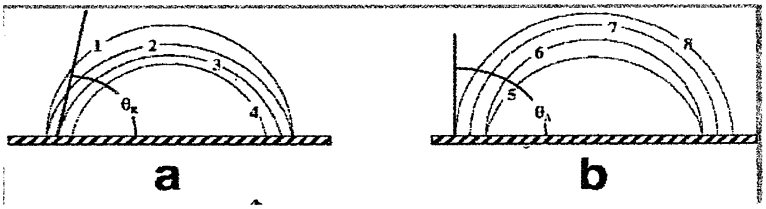

Figure 2.8 The addition or removal of liquid while determinating of advancing and receding contact angles [101].

An angle between the advancing and receding angle can be taken, but one metastable drop does not give as much information compared to determining both advancing and receding angles. The one metastable drop's contact angle will be somewhere in between the advancing and receding contact angles [101]. According to Pease in 1945, hysteresis is only a one dimensional problem that is caused by contact line structure [102].

2.2.4 Contact Angle Titrations

Contact angles can provide information about a wide range of surface chemistry characteristics. Contact angle titrations involve contact angle measurements using buffered (phosphate buffer solution) and unbuffered (water) aqueous solutions at varying pHs. When unbuffered aqueous solutions are used, the number of carboxylic acids

present on the surface can be determined, because the system is buffered by the carboxylic acid groups present on the surface which are neutralized by the hydroxide ions. The amount of carboxylic acids present is determined when there are equal amounts of carboxylic acids and hydroxide ions. If buffered aqueous solutions like a phosphate buffer solution at varying pHs are used, the pK_a of the substrate surface can be estimated by using data presented by the contact angle versus pH graph. Buffered solutions are used to remove the carboxylic acid groups influence on the pH of the drop. It has been determined that as the pH of an aqueous solution increases, a surface containing carboxylic acids will become more hydrophilic because the carboxylic acid groups are being ionized to carboxylate groups. At the inflection point on the contact angle vs pH graph using buffered solutions, there are equal amounts of carboxylic acid groups and carboxylate groups [103].

2.2.5 Conclusion

Contact angles can be used for determining many different aspects of surface chemistry. It can be used to determine whether a surface is hydrophilic or hydrophobic using water, or if multiple liquids with known surface tension are used, the surface tension of the solid can be calculated.

2.3 Attenuated Total Reflectance Infrared Spectroscopy (ATR-IR)

The first theory behind attenuated total reflection came from an observation from Newton that the spreading of a radiation wave at an interface between two different refractive indices mediums will experience total internal reflection. When a radiation wave undergoes total internal reflection, it is the basis of attenuated total reflection. In the 1960s more research was done by Harrick [104] and Fahrenfort [108] to increase

knowledge of applying internal total reflection to determine absorption spectra of different materials and compounds [104].

2.3.1 Theory

Attenuated total reflectance infrared spectroscopy is used to analyze the surface of a sample. The method for ATR-FTIR is for the sample to be in contact with the crystal, and the light passes through the crystal interacting with the sample [104]. It is based on total internal reflectance which occurs when a radiation beam enters the crystal and the incidence angle at the sample and crystal interface is greater than critical angle (refractive angle) [105]. The incidence angle at the sample and crystal interface is higher because the radiation beam is going from a medium having a high refractive index to one with a lower refractive index. When the incidence angle and critical angle are equal to 90° the light will be totally reflected which allows for more light to be reflected back into the high refractive index medium. The infrared light will bounce through the crystal to a detector, and then the spectrum is produced for analysis as depicted in figure 2.9 [104, 105].

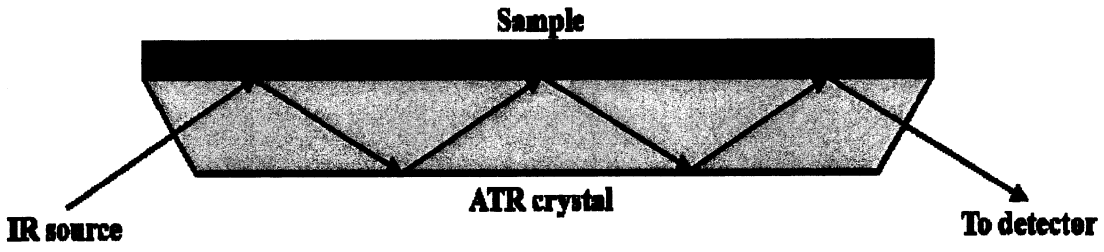

Figure 2.9 Schematic of ATR-FTIR [105].

Different molecules can be differentiated on the surface of a sample because the molecules absorb a light at a specific wavelength based on its composition. Some common crystals used in ATR-FTIR include zinc selenide, germanium, and thallium-iodide [105]. Since this technique is used for surface analysis, it can penetrate into different surface depths. If there is perfect contact between the crystal and surface, the light will penetrate the sample about one wavelength deep. When the incident angles are increased, the depths the light can penetrate will decrease [106].

2.3.2 Advantages and Disadvantages

The advantages of ATR-FTIR are the ability to determine surface characteristics and its sensitivity in doing so as well as the ability to calculate extinction coefficients without knowing the thickness of a sample [104, 109]. The disadvantages deal with the operation of the ATR-FTIR. When normalizing spectra, the band of interest and the normalization band should be fairly close, and if the bands do overlap, there will be band distortions and changes in intensities. The two bands need to be close because of the depth of the light into the sample is dependent on the wavelength. Another problem with this technique is the band maximum frequency shift due to dispersion across the absorption band which becomes important when determining the difference between a thin surface layer and the bulk of a sample. Lastly, is the possibility of artifacts in the spectra [104].

2.3.3 Conclusion

ATR-FTIR can be used to determine the composition of a sample surface. Since molecules vibrate and bend at different wavelengths, the different compounds present can be distinguished. For this research, ATR-FTIR was used to verify the presence of

carboxylic acids present on the PDMS surface and the effects of cell media on PDMS surface after modification.

2.4 Ultra-Violet/Visible Spectroscopy

Ultra-violet/visible (UV/VIS) spectroscopy is based on the Bouguer-Lambert-Beer law which was established based on discoveries from Pierre Bouguer in 1729, Johann Lambert in 1760, and August Beer in 1852 [112-114]. In 1792, Bouguer discovered that the amount of light that passes through a liquid sample will decrease with increasing sample thickness [112]. Johann Lambert in 1760 established the law of adsorption involving a logarithmic dependence of light transmission through a liquid sample, an absorption coefficient, and the distance light moves through the sample [113]. Lastly in 1852, August Beer determined that the amount of light absorbed from a liquid sample was proportional to the amount of solute in the sample [114]. By combining these three discoveries the Bouguer-Lambert-Beer law or Beer-Lambert law was established to be the following equation:

$$A = \varepsilon \ell c$$

where A is the absorbance (dimensionless), ε is the absorption coefficient (L mol^{-1} cm^{-1}), ℓ is the path length (cm), and c is the concentration of the liquid sample (M) [115]. As ascertained from the dates of discovery, UV/VIS is one of the oldest methods in spectroscopy. Other important historical discoveries for UV/VIS include the transition from colorimetry to photometry and finally to spectrophotometry which occurred due to the creation of detectors. The detectors started out using the human eye then to a photo element and photocell followed by a photomultiplier, and finally the most recent creation of the silicon diode detector [116].

2.4.1 Theory

The electromagnetic spectrum for UV/VIS range consists of wavelengths from 1000 – 8000 Å. The visible wavelength spectrum, 4000 – 8000 Å, the near ultra-violet spectrum, 2000 – 4000 Å, and the far ultra-violet spectrum are used for analyzing compounds. There are two types of spectra including emission spectra and absorption spectra. The emission spectra consist of the emitted light being analyzed, and the absorption spectra is obtained from the light being absorbed by a sample and then transmitted to a detector. When the molecule absorbs the light, the energy of the molecule increases which can occur in its electronic, vibrational, or rotational energy state. Before the molecule absorbs energy, it is said to be in a ground electronic state. The higher energy states are considered excited states. For every electronic state there is a ground state and a vibrational state, and for every vibrational state there is a ground and rotational state. When the molecule absorbs energy causing it the jump to an excited state, there are also changes in the electron distribution in the molecule. If the molecule is exposed to light from the far infrared region, it will cause a change in rotation energy; however, if it is exposed to light from the ultra-violet region, energy changes will occur in electronic, vibrational, and rotational energies [117].

When it comes to the possible electronic transitions that occur, there are selection rules that determine which can and cannot occur. The first rule determines semi-forbidden transitions, the second rule states singlet-triplet transitions should be forbidden, and the last rule determines forbidden transitions based on state symmetry. Even though some transitions are considered forbidden, they can be seen due to perturbations within the molecule and/or vibrational interactions [117].

Spectroscopic information can be obtained from samples in solution or as a solid depending on the attachments for the spectrophotometer. For a chemist, most samples are tested in solution which causes a loss of vibrational and rotational data. However, if a non-polar solvent is used, there is less of a change in absorption. Also, the solvent cannot absorb in the same region as the solute being tested. The solution to be analyzed is placed into a sample cell which can consist of either glass or quartz and can be different thicknesses from 0.1 cm to 10 cm with 1 cm being the most commonly used. Quartz sample cells may be used for most regions of the spectrum, but the glass sample cells can only be used for the visible region [117].

The basic components of a spectrometer are the light source, sample container, monochromator, and detector [117]. The light source can either be deuterium lamp for UV region or a tungsten lamp for VIS region [116]. The monochromator is either a prism or grating. The possible prisms include calcium fluoride or lithium fluoride for ultra-violet region, quartz for near ultra-violet region, and glass for the visible region [117]. Presently, mostly gratings are used as the monochromator, because gratings have a liner dispersion with wavelength affecting resolving power [116]. Detectors used include photographic plate, photoelectric cell, or more commonly a diode detector [116, 117].

2.4.2 Methylene Blue

Chromophores are groups in a compound that cause the sample to be colored which include C=C, C=O, and N=N, etc. However, some groups alone do not cause color unless a group called auxochromes is present which include C—Br, C—OH, and C-NH_2, etc. [117]. It is the chromophores and/or auxochromes which absorb the light.

Methylene blue is a penothiazinium dye which was first synthesized during the 19th century [118]. It is a basic cationic dye that attaches to acidic groups and absorbs at a wavelength of 666 nm when present as a monomer [118, 119]. There is a 1:1 ratio between the number of methylene blue monomers and the number of acidic groups present.

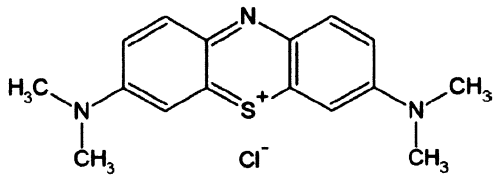

Figure 2.10 Structure of Methylene Blue Dye [119].

CHAPTER 3

EXPERIMENTAL

3.1 Chemicals and Reagents

Sylgard-184 silicone elastomer base and curing agent were obtained from Dow Corning Corporation, Midland, MI. Methylene blue dye solid was obtained from Acros Organics, Geel, Belgium. ACS certified monosodium phosphate, disodium phosphate, LB powder, and propidium iodide solid were obtained from Fisher Scientific, Waltham, MA. The metal stencil was obtained from Small Parts, Inc, Miami Lakes, FL. *Escherichia coli* where obtained from Dr. Roger Cruz-Vera (W3110) and Dr. Robert McFeeters (BL-21).

3.2 PDMS Preparation and Irradiation

The Sylgard-184 elastomer base and curing agent were mixed in a 10:1 ratio by weight, respectively. The base and curing agent were mixed together for roughly two minutes in a disposable cup. Once the elastomer was thoroughly mixed, it was poured into a petri dish and placed into a vacuum chamber for approximately one minute to assist in the removal of air bubbles. To cure, the petri dish was left on a counter in ambient conditions for 24 hours or it was placed on a hot plate at 65°C for 2-3 hours.

The cured PDMS was then cut into small rectangular pieces. For irradiation of the PDMS pieces, a mercury lamp produced by USHIO American Inc., Cyprus, California was used. The irradiation setup can be seen in figure 3.1.

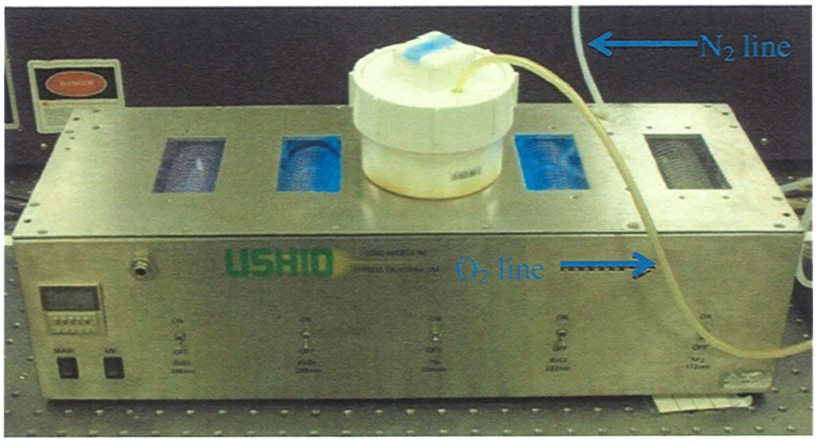

Figure 3.1 PDMS irradiation setup [85].

Sample irradiation was accomplished by placing the sample onto a glass slide facing the lamp. Small binder clips attached the sample to the slide at each end creating a distance of 2 mm between the lamp and samples. A PVC container covered the glass slide holding the samples. The contained environment around the PDMS coupons was purged for 15 minutes with ultra-high purity oxygen at a flow rate of approximately 2 L/min to ensure an oxygen rich environment. After 15 minutes of purging, the mercury lamp was turned on exposing the PDMS samples to 254 nm mercury radiation at fluence of 13 mW/cm^2. The samples were irradiated for 15 minutes, 30 minutes, 45 minutes, 60

minutes, 75 minutes, and 90 minutes. After irradiation, the PDMS pieces were stored in a 50 % acetic acid solution until needed.

3.3 *E. coli* Growth

The *E. coli* strain used was BL-21 which contained the pGlub plasmid. They were grown overnight from a colony on an agar plate with carbenicillin. The colony was picked from the plate and placed in 3 mL of LB media and 3 μL of carbenicillin (100 μg/mL), and allowed to grow for 16 hours in a shaking incubator at 37°C. Approximately 18 hours later, 1 mL of cells was centrifuged for 20 seconds using an Eppendorf Brinkman Centrifuge 5414, and the supernatant removed. A fresh 3 mL of LB media with 3 μL of carbenicillin was prepared. Then 500 μL of the fresh media was used to resuspend the pellet, but only 100 μL of the cells were transferred to the fresh LB media with antibiotics. These cells were allowed to grow in a shaking incubator at 37°C for 8 hours at which point they were transferred to 3 mL M9 media with 3 μL carbenicillin the same way as mentioned above. The composition of M9 minimal media is located in the appendix. They were allowed to grow for 16 hours in a shaking incubator at 37 °C, and afterwards, the bacteria were transferred to fresh M9 media and antibotics depending on the experiment performed. For each experiment, the *E. coli* were grown to an OD_{600} of 0.5 – 0.7, and at that point, the cells were removed from the shaking incubator and prepared for that particular experiment. Stock cultures were made from *E. coli* grown to an OD_{600} of 1, and then 1 mL of cells and 300 μL of 80 % glycerol were combined and mixed well in a 1.5 mL centrifuge tube.

Cultures were also grown using frozen stock culture by thawing the frozen stock culture and placing into fresh media with antibiotics with the number of frozen stock needed depending on the size of the experiment.

3.4 *E. coli* Attachment

In order to attach the *E. coli* to the PDMS, 10 mL of *E. coli* culture were placed into a 15 mL Falcon™ tube. The irradiated PDMS samples were removed from the 50 % acetic acid solution, rinsed with deionized water, and placed into the *E. coli* culture for approximately one hour at room temerature. The cap was placed on the Falcon tube to seal it. For the pH experiment, the pH of the media was adjusted using 20 % HCl and/or 1 M NaOH. The range of pH tested was pH 7 – pH 2. After the pieces were placed in the media for one hour, they were removed, rinsed with deionized water, and briefly dried with a light nitrogen flow. The pieces were placed in petri dishes to finish drying overnight.

3.4.1 Propidium Iodide

Propidium iodide, PI, is used to stain dead cells as well as determine membrane integrity. PI will only diffuse through dead cells' membranes since living cells can exclude this compound [111]. The method from Molecular Probes was used [110]. A stock solution of PI was made containing 1 mg/mL in deionized water and was protected from light and stored at 4°C. From the stock solution, a working solution with a 1.5 μM concentration was made using a ratio of 1:1000 of stock solution and PBS, respectively. After cell attachment procedure and drying the surface using nitrogen flow, the cells were stained by placing 300 μL of working stain solution on the sample and covering the sample with a coverslip to ensure the stain spread evenly over the surface. The sample

was incubated for 30 minutes in a dark room. The coverslip was then removed to rinse the sample with PBS removing any unbound dye, and then a new coverslip was placed on the sample. The sample was viewed under a laser scanning confocal microscope.

3.5 Visualization of Cell Attachment

The cells were viewed under a laser scanning confocal microscope, Zeiss LSM 700, which can be seen in figure 3.2. *E. coli* was viewed using 10X and 63X oil immersion magnification. The 63X magnification images were taken with an area of 175 μm X 175 μm or 123 μm X 123 μm depending on the experiment. To obtain a fluorescent image of dead cells, propidium iodide was selected, and the master gain was adjusted to visualize the red fluorescent cells. For each sample, 5 – 10 images were taken for analysis. After the images were taken, cells in the image were counted using the NIH Image J program. The image was opened in the program, and the cell count plugin was opened as well. In the cell count plugin box, the image was initialized and the type I cell counter was selected. Afterwards, each location of a cell was clicked counting the number of cells next to the type of counter chosen.

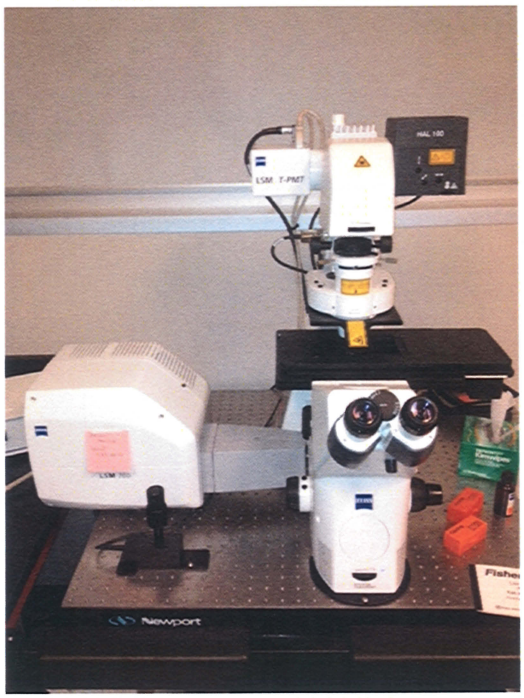

Figure 3.2 Zeiss LSM 700 confocal microscope.

3.6 ATR-FTIR

The infrared spectra were obtained using a Perkin Elmer Spectrum One Fourier Transform Infrared Spectrometer with a built in attenuated total reflectance accessory as seen in figure 3.3. For each spectra, the pressure arm was adjusted to a force of ~50, 32 scans were taken, and the region analyzed was 4000 – 500 cm^{-1}.

Figure 3.3 ATR-FTIR instrument [85].

3.7 Contact Angle Measurements

Contact angles were measured using a Rame Hart goniometer (model 50-00/100-00) that is fitted with a Sony XCD-X700-1.05 camera as seen in figure 3.4. The contact angle measurements were done using the sessile drop technique where a micropipette was used to dispense a 4 μL drop of a test liquid onto the sample. Six to eight drops were placed at different points on the sample. An image of the drop on the surface was captured using Fire I software. Image J software was then used to enhance the surface contrast, identify the edges, and to measure the contact angle using Drop Snake [120]. Contact angle measurements were done for PDMS pieces irradiated at 75 minutes and placed in M9 or LB media at pH 7 or pH 2 using deionized water as the test liquid. Contact angle titrations were also completed using PDMS pieces irradiated at 75 minutes. The solutions used were a phosphate buffer at pH 2, 4, 6, 8, and 10. The test liquid was

used on PDMS coupons that had been placed in media at varying pHs (2-7) as well as coupons that were not placed in media. For each pH of the buffered solution, three pieces of PDMS were tested. For the pieces that were placed in media at different pH, each buffered solution at a different pH was tested.

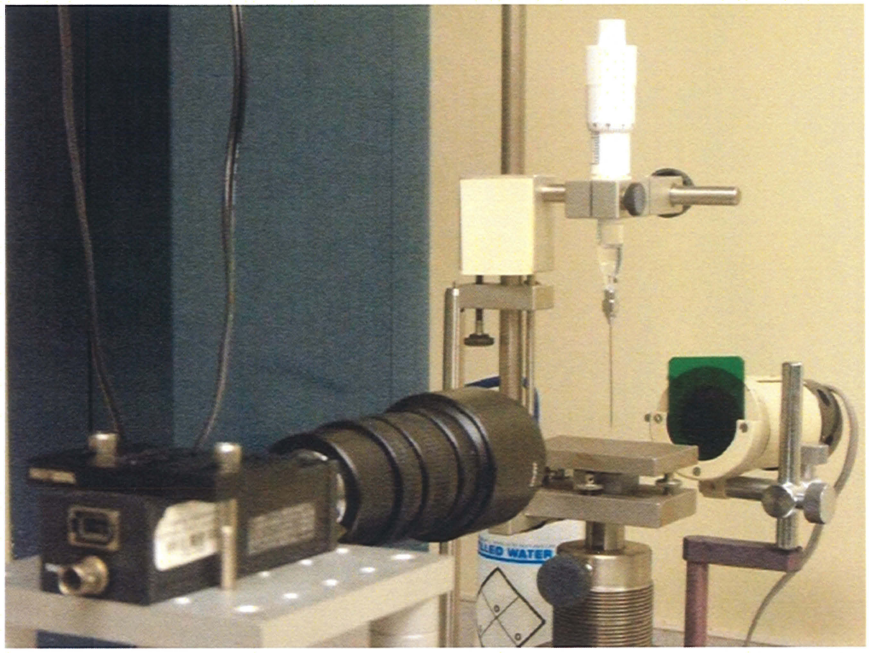

Figure 3.4 Contact angle setup [85].

3.8 Methylene Blue

Methylene blue dye was used to determine the number of carboxylic acids present on the surface of irradiated PDMS after being placed in LB media and M9 media. The PDMS pieces were cut into a circle with a diameter of 1.2 cm, and then irradiated for 75 minutes. The samples were placed into either LB media or M9 media at different pHs

and immersed for an hour. Afterwards, they were removed, rinsed with deionized water, and placed into a pH 10, 0.5 mM methylene blue solution for 6 hours at room temperature. The samples were removed after the 6 hours, rinsed very well with deionized water to remove any unbound methylene blue dye, and placed into 3 mL of a 50 % acetic acid solution. The 50 % acetic acid solution desorbs the methylene dye from the carboxylic acids. The methylene blue is measured at 666 nm. The absorbance of the 50 % acetic acid solution was taken using a HP 8452 diode array UV/VIS spectrophotometer. A calibration curve of standardized methylene blue solutions versus absorbance was created. Using the equation of the linear fit of the calibration curve, the concentration of methylene blue was determined. The ratio of methylene blue to carboxylic acids is 1:1, so from the number of carboxylic acids and the surface area of the PDMS, the concentration of carboxylic acids was calculated.

CHAPTER 4

RESULTS AND DISCUSSION

4.1 Effect of Media on Cell Attachment

The objective of this research was to develop a method to attach BL-21 *E. coli* to the surface of a modified piece of PDMS via surface bound carboxylic acids. From previous research, it was determined that the greatest amount of carboxylic acids present on a PDMS surface occurred after an irradiation time of 75 minutes. Since *E. coli* cells are one of the easiest bacteria to obtain and grow, it was chosen as the organism to use for this research. The results of growing *E. coli* in various medias can be seen in the following figures. In figure 4.1, there is little to no attachment of BL-21 cells grown in LB media at pH 7 and pH 2.

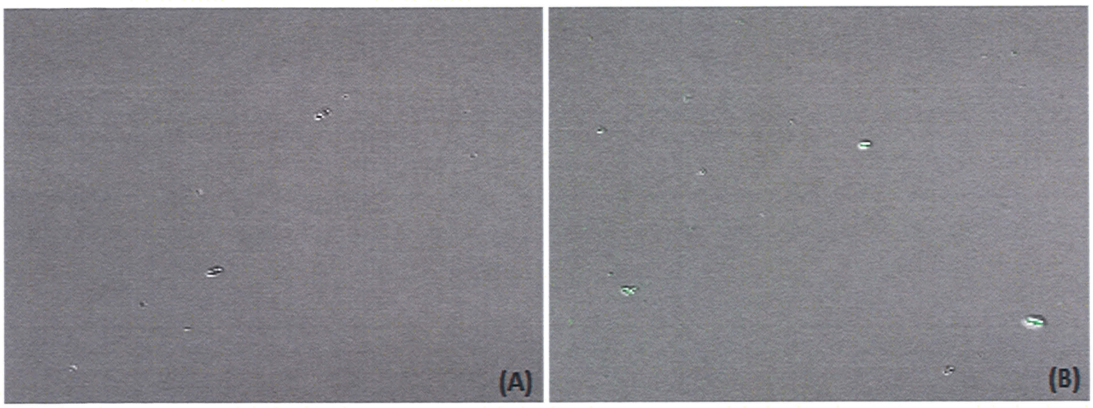

Figure 4.1 *E. coli* culture grown in LB media and exposed to irradiated PDMS. (A) represents an image of an irradiated PDMS coupon after being placed in pH 7 LB media. (B) represents an irradiated PDMS coupon after being placed in LB media adjusted to pH 2 after cells had grown to desired OD. Both coupons were allowed to sit in the culture for one hour and rinsed with deionized water.

As a control, a native PDMS piece was also tested using LB media at pH 7 and pH 2. In figure 4.2, it can be seen, there is little to no attachment on native PDMS as well.

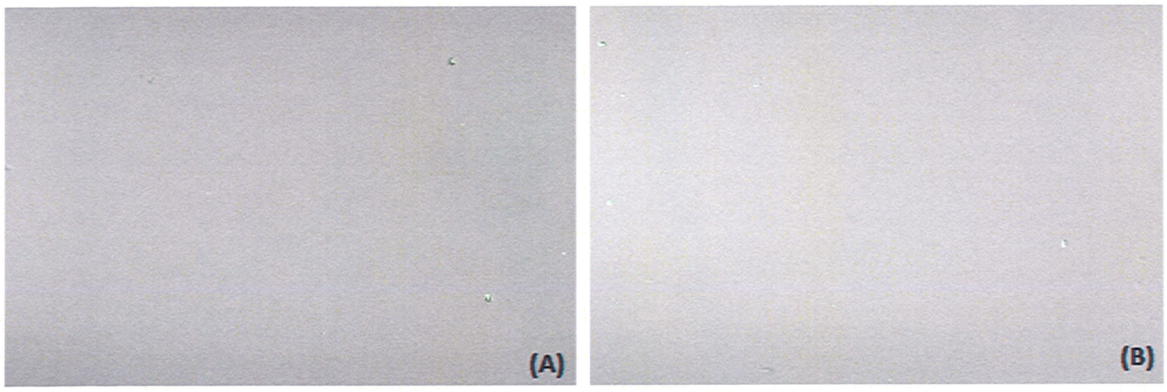

Figure 4.2 *E. coli* grown in LB media and exposed to native PDMS. (A) shows a native PDMS coupon after being placed in pH 7 LB media, and (B) shows a native PDMS coupon after being placed in pH 2 LB media. Both coupons were placed in culture for one hour and rinsed with deionized water.

Since no attachment of BL-21 *E. coli* were seen using LB media, M9 minimal media was used, and the results are depicted in figure 4.3 which reveals significant attachment at pH 2.

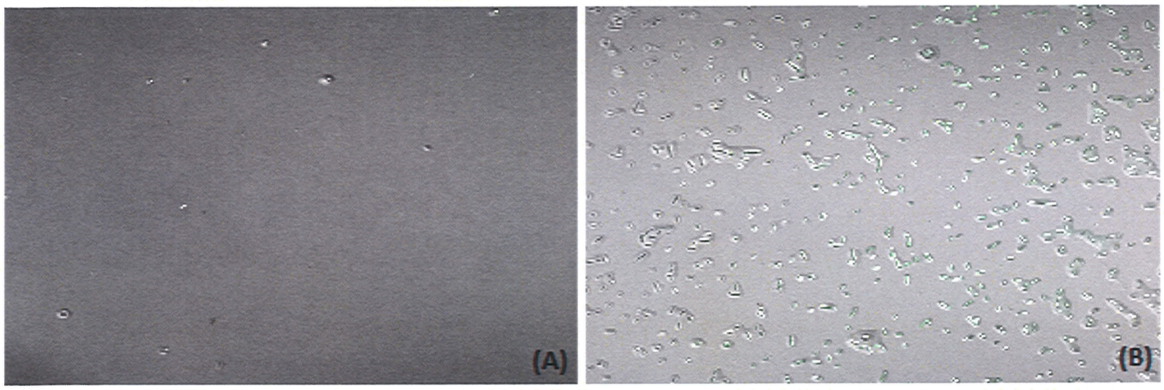

Figure 4.3 *E. coli* grown in M9 media and exposed to irradiated PDMS. (A) represents irradiated PDMS placed in pH 7 M9 media culture. (B) represents irradiated PDMS placed in M9 media culture adjusted to pH 2. PDMS coupons placed in culture for one hour and rinsed with deionized water.

Again, native coupons of PDMS were tested using M9 media at pH 7 and pH2. The results can be seen in figure 4.4 which also shows attachment at pH 2.

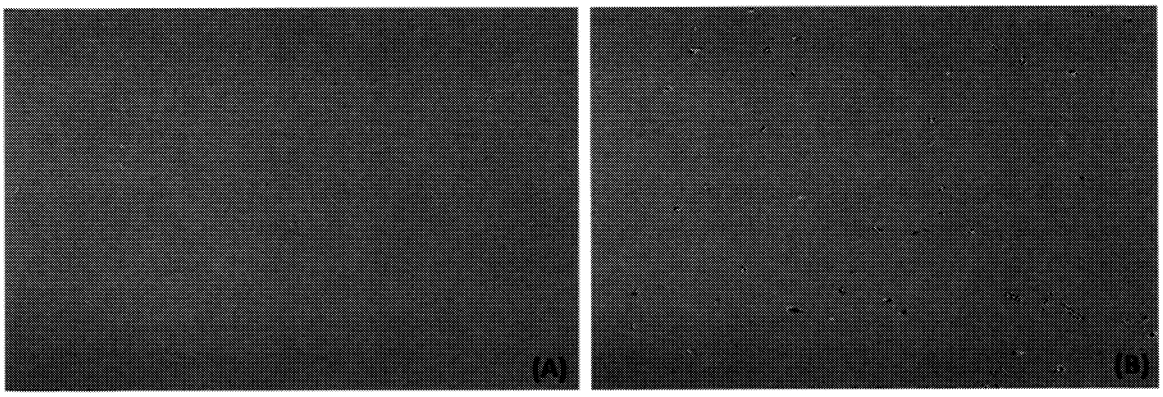

Figure 4.4 *E. coli* grown in M9 media and exposed to native PDMS. In (A) the media was at pH 7, and in (B) the media pH was adjusted to 2. Native PDMS coupons were placed in the different pH media for one hour and rinsed with deionized water.

The results indicate that the *E. coli* are capable of attaching to the irradiated and native PDMS surfaces at an acidic pH. The cell attachment occurring at an acidic pH coincides with previous results showing the relation of surface carboxylic acid groups requiring acidic conditions. These results in combination with the previous results indicate that the best pH was an acidic one and the best media was the M9 minimal media. The M9 media allowed cell attachment because it only consists of phosphates, salts, vitamins, and glucose compared to the rich components of LB media which possibly affect attachment.

4.2 Effect of pH and Irradiation Time on Cell Attachment

The results appear to indicate there is a pH dependence on cell attachment. This supposition coincides with the presence of carboxylic acids on the irradiated PDMS surface. Dharmarajan's previous work indicates that acidic conditions prevent the rotation of the carboxylic groups back to the bulk of the polymer. In order to support the hypothesis that *E. coli* attachment is dependent on pH, pH 2 – 7 were tested to determine the effects on cell attachment. The pH experiment was performed three separate times by

growing *E. coli* in M9 media from a plate colony, using two pieces of PDMS, and taking 10 images per PDMS coupon. A set of representative images for the pH experiment can be seen in figure 4.5.

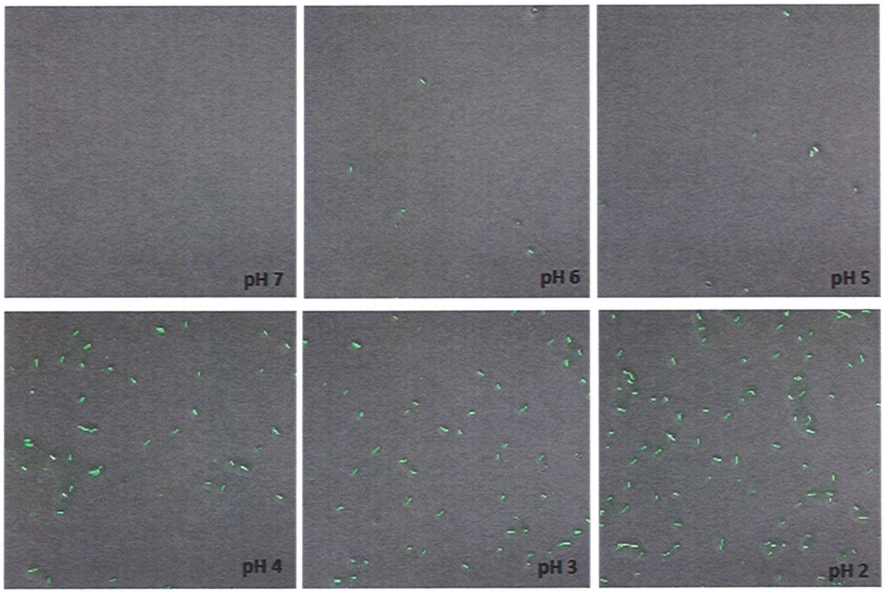

Figure 4.5 Images depicting the different amount of cell attachment at pH values 7 – 2. The irradiated PDMS coupons were placed in *E. coli* M9 culture for one hour, removed, and rinsed with deionized water. The pH was adjusted after the cells had grown to the desired OD_{600} of 0.5 – 0.7.

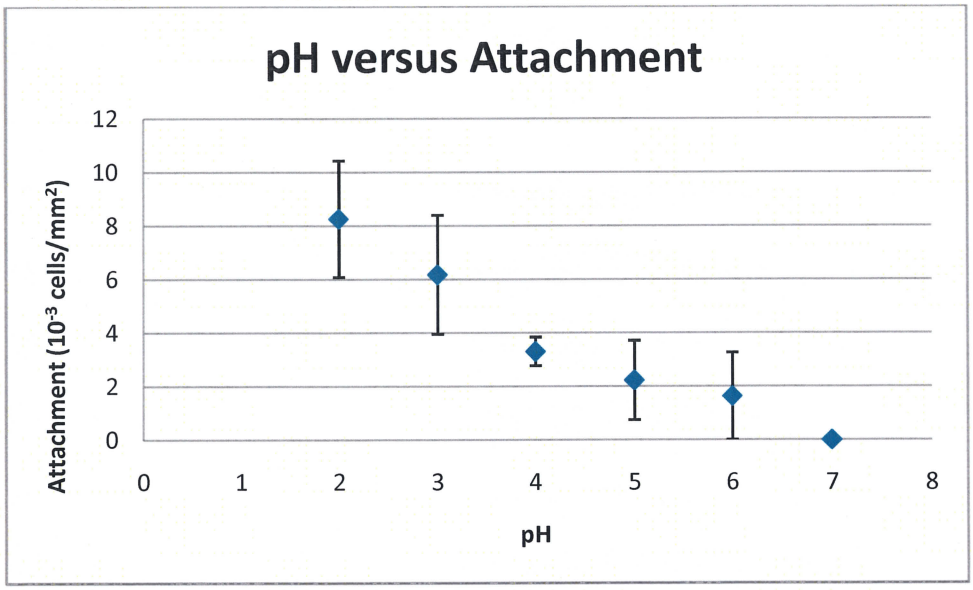

Figure 4.6 The amount of BL-21 cells per mm^2 attached to a PDMS surface irradiated for 75 minutes.

This experiment determined the lowest pH measured for attachment was a pH of 2; however, at this pH the cells are in an unhealthy environment and ultimately dead. There appears to be a linear decrease of cell attachment as the pH increases that can be seen in figure 4.6. It is believed that the *E. coli* are attaching to the carboxylic acids present on the surface of the modified PDMS which agrees with the results that indicate the relation of carboxylic acids at an acidic pH.

The method for bacterial attachment in this research is a general one that can be used to test different bacteria. For this research, the parent strain, W3110, of the *E. coli* strain used throughout this research was also tested to determine if the same pH dependence would be observed.

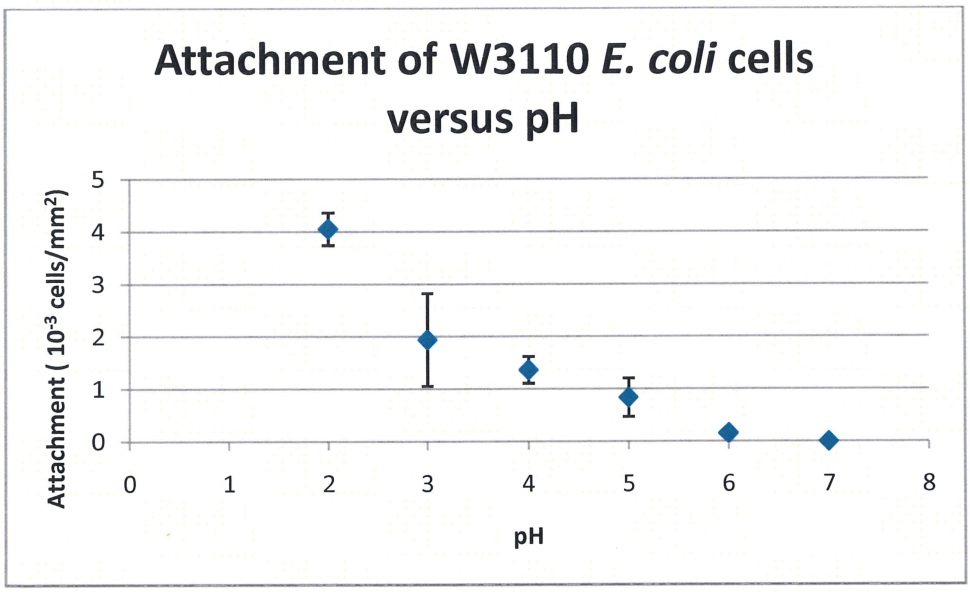

Figure 4.7 The amount of W3110 cells per mm^2 with varying pH on PDMS irradiated for 75 minutes.

The W3110 strain of *E. coli* showed the same trend with regard to the amount of attachment with varying pH which can be seen in figure 4.7. The best attachment also occurred at the acidic condition of pH 2.

When establishing the optimal media to be used during these experiments, native PDMS was also examined for cell attachment. In order to determine if there was a relationship between media pH and attachment of cells to the native PDMS surface, the media with adjusted pH 2 – 7 were tested to determine the amount of cell attachment.

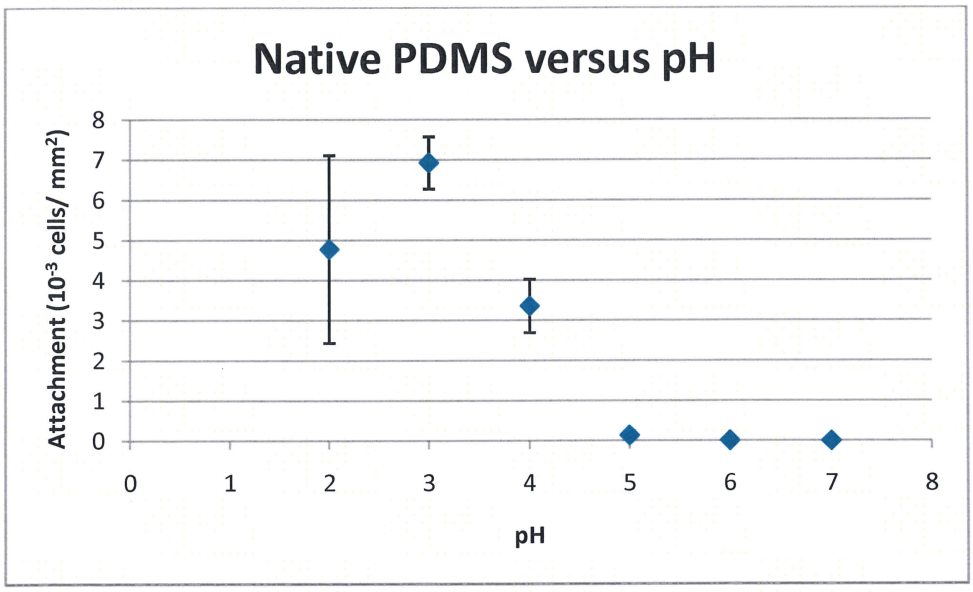

Figure 4.8 Amount of BL-21 cell attached to a native PDMS while varying the pH of the M9 culture. The error bars for pH 6 and 7 are zero, because no attachment was seen. For pH 5, the standard deviation was ± 0.10269.

The amount of cell attachment to a native PDMS surface was determined to be pH dependent, because attachment was only seen at relatively high acidic pHs which can be seen in figure 4.8. The greatest amount of attachment was seen at pH 2 and pH 3 which is in some agreement with cell attachment for irradiated PDMS which exhibits the highest amount of attachment at pH 2. The previous results seem to indicate a correlation between attachment and pH of the media. However, experiments with native PDMS seem to indicate no correlation between surface carboxylic groups and attachment.

Previous research has shown that as the irradiation time increases up to 75 minutes, the amount of carboxylic acids increases as well. After 75 minutes, a glassy layer forms on the PDMS surface due to degradation of the polymer backbone [85]. To determine if the amount of carboxylic acids present on the surface affect cell attachment,

the amount of irradiation was also varied to help determine if attachment was occurring through the carboxylic acids. Each irradiation time was tested three times each using BL-21 *E. coli* culture grown from a plate.

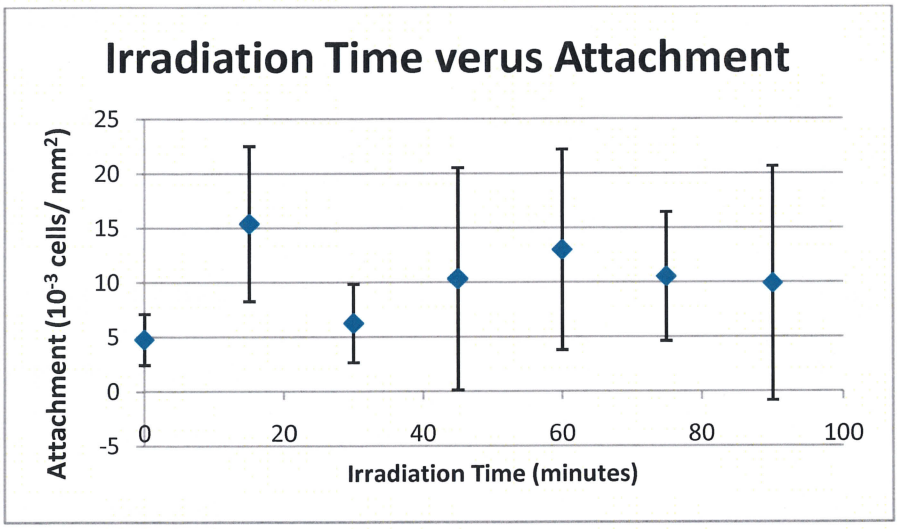

Figure 4.9 Amount of BL-21 cells per mm^2 for each irradiation time tested. Coupons of PDMS were irradiated at 15 minute intervals from 0 – 90 minutes. Each coupon was placed in M9 culture adjusted to pH 2. This experiment was repeated three times using two coupons of irradiated PDMS. For each coupon, ten images (123 μm x 123 μm or 172 μm x 172 μm) were taken from each which was used to count cells in the image.

In figure 4.9, the degree of cell attachment with respect to different irradiation times is roughly constant. Given that there is constant attachment no matter the irradiation time indicates the *E. coli* may not need as many carboxylic acids for attachment compared to what is present on the surface. The native PDMS shows a small amount of attachment, but not as much attachment compared to the different irradiation times containing carboxylic acids. This experiment was done at a pH of 2 which is an unhealthy

environment for the bacteria. When *E. coli* are placed in this type of condition, they tend to require closeness to one another which would explain the high standard deviation in the amount of cell attachment per different irradiation times. The clumping of *E. coli* cells is different from experiment to experiment. Also, cracking may contribute to the high standard deviation for irradiation ties of 60, 75, and 90 minutes. After 75 minutes, a glassy layer forms due to polymer backbone degradation [85].

4.3 Effect of Culture Methods on Attachment

Two methods for growing *E. coli* were utilized in this work. Frozen stock cultures were used to grow *E. coli* cultures for experiments as well as growing *E. coli* using a plate colony. Upon utilization of frozen stock culture, there is no mechanism of determining how many dead cells are already present or the number of possible mutations that have occurred even though the culture is growing. During the manufacture of frozen stock cultures it is imperative that the glycerol completely mixes with the cells, otherwise the bacteria will die once placed in the freezer. An experiment was performed where two cultures were grown simultaneously with one using frozen stock cultures and the other from a plate. PDMS coupons were irradiated for 75 minutes and the pH of the cultures was changed to pH 2. After counting cells, it was determined that both PDMS pieces contained roughly the same amount of cells, but the frozen stock cultures had a higher standard deviation compared to those using a plate colony. This supports the argument that *E. coli* are healthier when grown from a plate colony than when grown from a frozen stock culture. The number of dead cells attached to a PDMS surface irradiated for 75 minutes and placed in varying pH M9 media was determined by staining the samples with propidium iodide which only penetrates cell membranes of dead bacteria. Stained

cells fluoresce red. It was determined that all cells attached were dead, regardless of pH. A representative image showing the *E. coli* fluorescing red can be seen in figure 4.10.

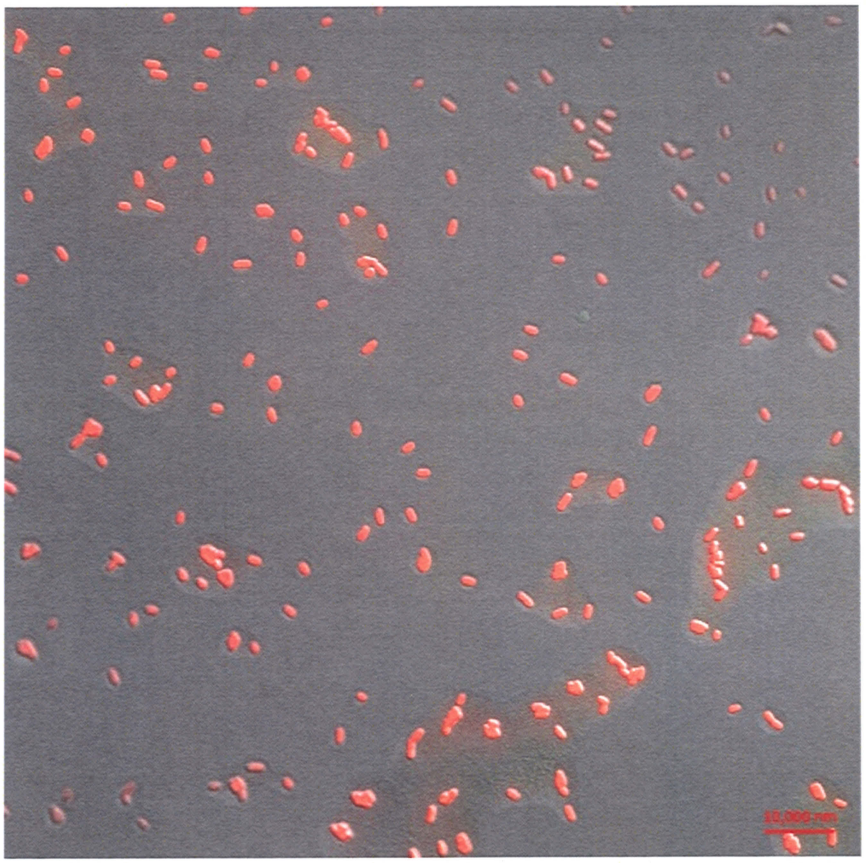

Figure 4.10 *E. coli* cells stained with propidium iodide. A PDMS piece was irradiated for 75 minutes and placed in a pH2 M9 cell culture. All cells fluoresced red indicating the cells were dead.

4.4 Quantification of Carboxylic Acids

The results for cell attachment seemed to indicate that there is not a strong correlation between the number of carboxylic acids present and the amount of *E. coli* attachment. It also showed that there is pH dependence for cell attachment on native and

irradiated PDMS surfaces. To verify and characterize the presence of carboxylic acids on the surface of irradiated PDMS, a methylene blue experiment and contact angle titrations were performed. Methylene blue dye attaches to carboxylic acid groups meaning it will attach to carboxylic acids present on an irradiated PDMS surface. Previously, Dharmarajan used methylene blue dye to determine the amount of carboxylic acids present after different irradiation times. For a 75 minute irradiation, Dharmarajan determined there are 2.5×10^{16} molecules/cm^2 present on the surface [84]. Methylene blue was used to determine the amount of carboxylic acids present on the irradiated PDMS surface after being placed in LB or M9 media at varying pH. This experiment was performed to determine the amount of carboxylic acids present after being placed in the media to determine if there was a difference compared to regular irradiated PDMS, or if there was any difference in the attachment of media components to the carboxylic acids.

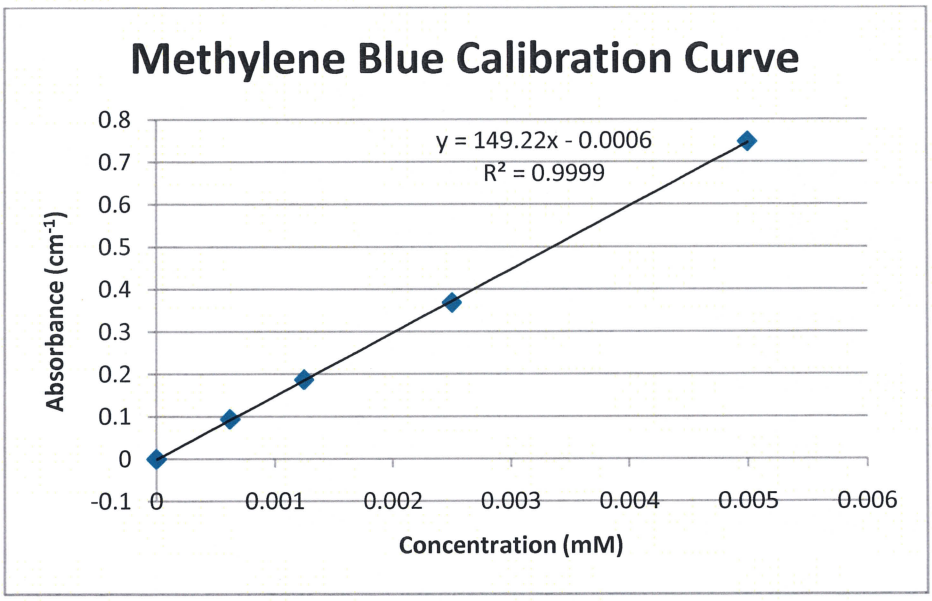

Figure 4.11 Methylene blue calibration curve used to determine the amount of carboxylic acids present on an irradiated PDMS surface after being placed in LB or M9 media.

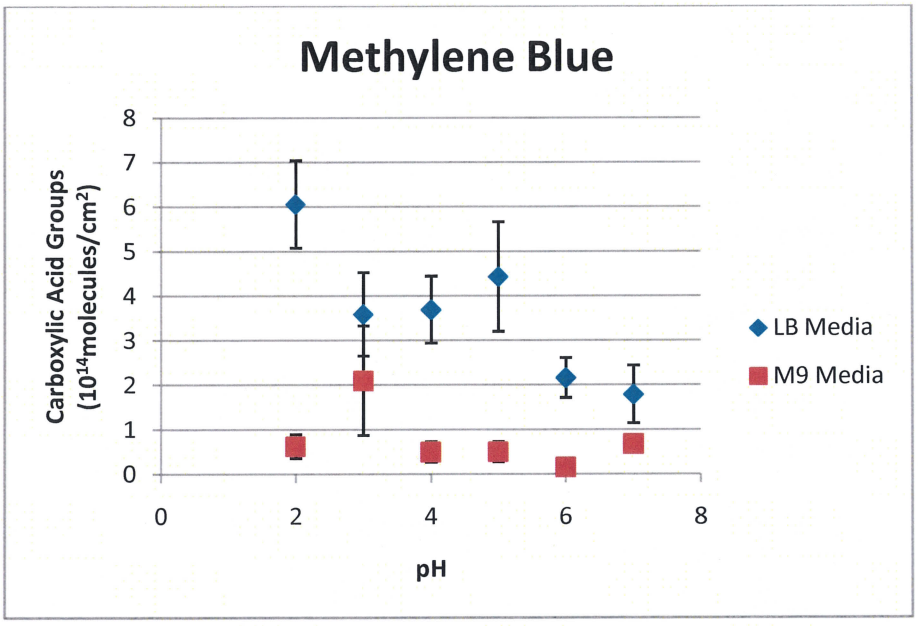

Figure 4.12 Amount of carboxylic acids present on the surface of PDMS irradiated for 75 minutes after being placed in LB or M9 media pH ranging from 2 – 7.

The methylene blue dye indicated that there were more carboxylic acids present on the PDMS surface after being placed in LB media compared to PDMS surfaces immersed in M9 media as indicated in figure 4.12. There are 2.5 x 10^{16} molecules/cm^2 for PDMS irradiated at 75 minutes. The media has a minimal interaction with the carboxylic acids present on the surface, because only one percent is being affected. The results of the methylene blue dye show the same results as the IR spectra which can be seen in figure 4.14. Both indicate the media components are not interacting with the carboxylic acids.

In order to verify the presence of carboxylic acids, a contact angle titration was performed on PDMS coupons that were irradiated for 75 minutes which can be seen in figure 4.13.

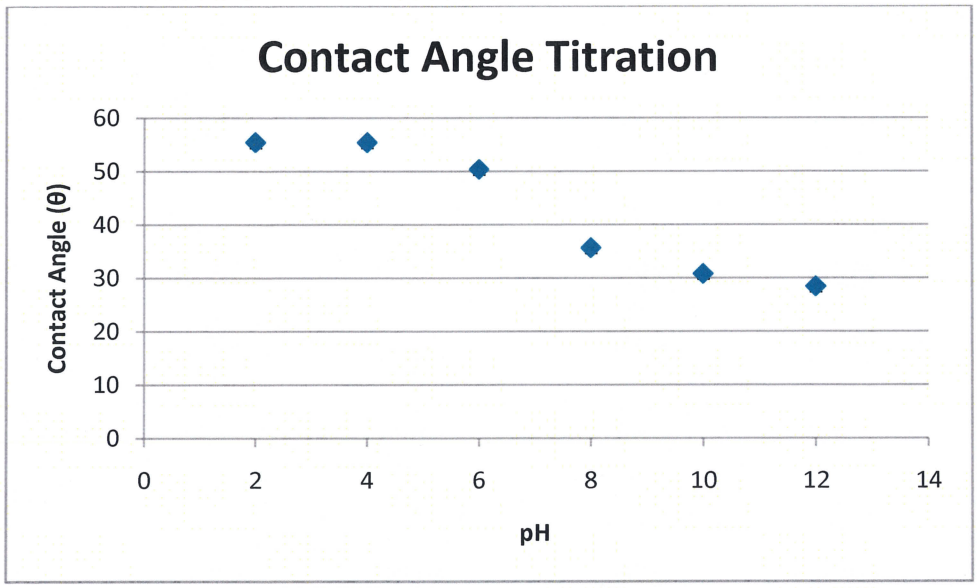

Figure 4.13 Contact angle titration of PDMS irradiated for 75 minutes. The liquid used for contact angles was 0.1 M phosphate buffer adjusted to the needed pH 2 - 12.

The contact angle titration was performed to verify carboxylic acids were present on the surface of the irradiated sample, and to estimate the pKa of the irradiated PDMS surface. From figure 4.13, the pKa can be estimated to be 7. The results are similar to those obtained by Holmes-Farley and colleagues, where the same contact angle titration was performed on polyethylene with carboxylic acids [103].

4.5 Effect of Media on Surface Chemistry of Irradiated and Native PDMS

ATR-FTIR was used to analyze the surface of modified PDMS after being in LB and M9 media, and the results can be seen in figure 4.14. After irradiated PDMS coupons were placed in either media the carbonyl peak at ~1715 cm^{-1} decreased, but the OH peak stayed roughly the same at 3000 cm^{-1}–3650 cm^{-1}. The glucose and vitamins present in M9 media contain hydroxyl and carboxylic acids that could attach to carboxylic acids present on the modified surface. However, when a modified piece of PDMS was place in M9 media with no vitamins and glucose, the same peaks were observed as irradiated PDMS placed in regular M9 media. There was no peak showing an ester formation which would be seen at 1765-1720 cm^{-1} with no OH peak visible [121]. The IR spectra of irradiated PDMS also verified the presence of carboxylic acids on the polymer surface.

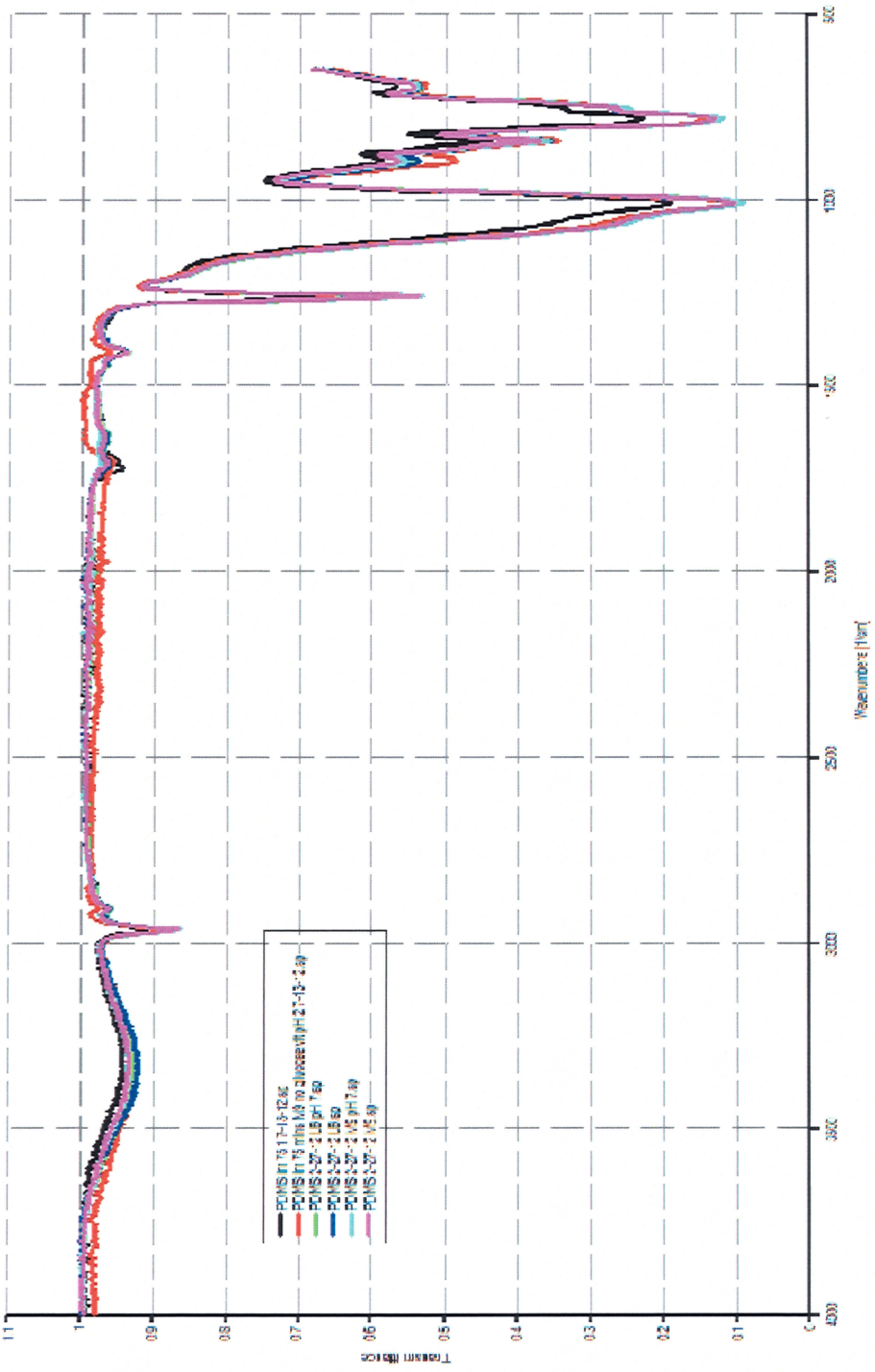

Figure 4.14 ATR-FTIR spectra of irradiated PDMS and after being placed in LB and M9 media at pH 2, pH 7, and without glucose and vitamins.

From the results obtained above, it is theorized that the *E. coli* attach to the modified PDMS using their outer membrane proteins and/or if the outer membrane is removed, peptidoglycan. Both the proteins and peptidoglycan contain amino acids that are capable of creating an electrostatic interaction with the carboxylic acids on the modified PDMS surface. The ATR-FTIR data does not show any reaction between the media components and the carboxylic acids.

The native PDMS also showed bacterial attachment at an acidic pH condition. To determine if the acidic pH was changing the surface chemistry of the native PDMS, ATR-FTIR data was obtained for a PDMS piece after being placed in 20% HCl and pH 2 M9 media with and without glucose and vitamins which would verify that no glucose or vitamins were attaching to the native surface. In figure 4.15, all spectra appeared the same as a native PDMS surface showing the pH condition was not affecting the surface and no glucose or vitamins were attaching. The *E. coli* are possibly attaching to the native PDMS due to surface roughness and/or the residual electrostatic charge present after removal from the petri dish.

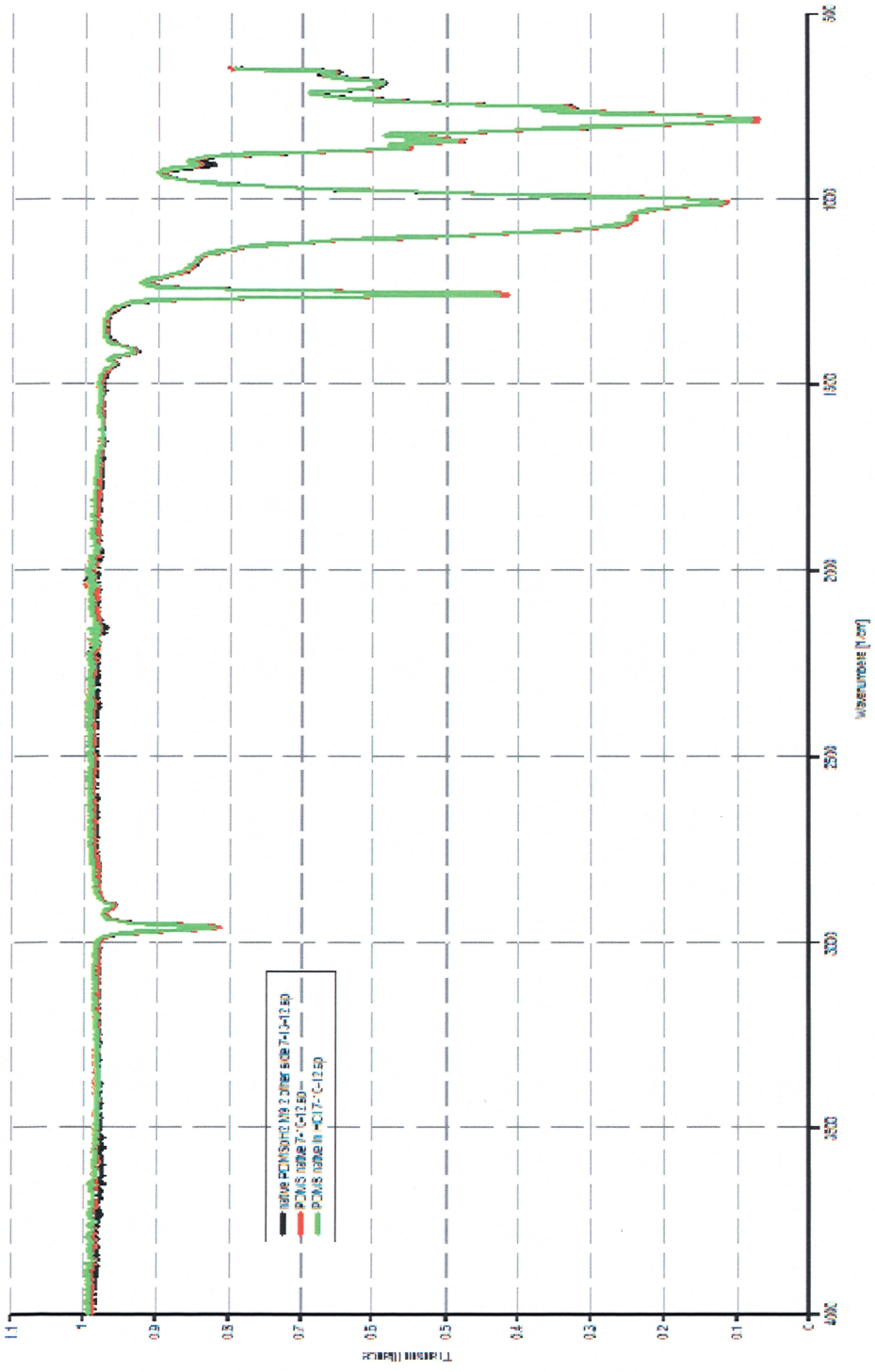

Figure 4.15 ATR-FTIR spectra of a native PDMS and after being placed in 20% HCl and pH 2 M9 media

CHAPTER 5

CONCLUSION

5.1 Summary

The understanding of bacterial cell attachment on PDMS can be insightful for many different aspects of science including chemistry and biology. In this research, a general method was developed for attachment of *E. coli* to native and modified PDMS surfaces. The method involves growing the *E. coli* to the needed optical density, placing the culture in a Falcon tube, putting the PDMS piece in the falcon tube for an hour, and then removing and rinsing with deionized water. Different pHs were tested to determine the most bacterial attachment which occurred at an acidic pH of 2. There was a roughly linear decrease in the amount of cell attachment with an increase in pH. Since it was theorized that the *E. coli* would be attaching to the carboxylic acids on the modified surface, different irradiation times were also tested because by varying the irradiation time, the amount of carboxylic acids vary as well. However, this result was not seen. The results showed to be equal attachment with all the irradiation times indicating the *E. coli* may not need many carboxylic acids for attachment. Native PDMS was tested for call attachment at pH 7 and pH 2 with only attachment seen at pH 2. Due to the possible

pH dependence on attachment, pH 2 – 7 were tested with *E. coli* only attaching to native PDMS surfaces at an acidic pH. To determine whether the *E. coli* were attaching to the carboxylic acids, ATR-FTIR data was done on different PDMS samples after being placed in different media solutions. For the irradiated PDMS pieces, they were placed in LB and M9 media at pH 7 and pH 2, with and without glucose and vitamins. When comparing these spectra, all appeared the same as the irradiated piece; however, there was a decrease in the carbonyl peak and the hydroxyl peak stayed roughly the same. For the native PDMS pieces, they were placed in 20% HCl, and M9 media at pH 2 with and without glucose and vitamins. These spectra were exactly the same as the native PDMS spectrum. From all the data in this research, the *E. coli* are theorized to be attaching to the PDMS surface by an electrostatic reaction with the lipopolysaccharide and/or proteins on the *E. coli* membrane.

5.2 Future Work

The method developed in this research can be optimized to increase bacterial viability when attached to the PDMS surface. The bacteria are grown in a shaking 37 °C incubator. Once the needed optical density is obtained, they are removed from the incubator to be left out at room temperature. Also, when the cells are grown in the incubator, the test tubes or flasks are not completely sealed so that so oxygen can enter the container. To allow for the cells to be healthier, once the optical density is reached, the cells can be placed in the test tubes used to grow smaller cultures instead of using the Falcon tubes. Also, the test tubes could be placed back into the incubator after changing the pH and/or adding in the PDMS. Throughout this research, the health of the cells has been found to be important. As the plate used for starting a culture is used for

experiments, the cells grow to the usual optical density at a slower rate than expected. There are some morphology changes including elongation, clumping, and unusual rod shapes. Also, there seems to be a difference in the possibility of clumping and morphology changes related to the optical density the culture is allowed to grow too. If the cells are grown to an optical density of roughly 0.5 there is a slim chance of the morphology changes if the plate's age is not older than a couple weeks. At an optical density of 0.7 or higher, there is a greater risk for morphology differences as well as when the PDMS is sitting in the falcon tube containing cells, the cells will fall out of solution into the bottom of the tube. The amount of time the PDMS soaks in the cell culture could also be changed because in literature anywhere from 20 minutes to overnight was done. Lastly, the effect of the *E. coli* membrane in the different medias needs to be investigated more. The cell membrane will vary with LB media and M9 media which could change the amount of attachment. These recommended changes in the method should increase the chance for live cells on the PDMS surface.

The PDMS has also been a factor in the attachment of *E. coli.* First, the age of the PDMS does affect the bacterial attachment. Preliminary results indicate that PDMS is usable for a week at which point it should be discarded. If the PDMS has been made, irradiated, and stored in 50 % acetic acid solution, results indicate it is usable for an indefinite time as long as fresh 50% acetic acid solution is added to the storage container periodically to replace solution lost to evaporation. To ensure a clean PDMS coupon, a fresh petri dish and the side facing down should be used. Lastly, previous research has shown that the carboxylic acids will rotate back into the bulk over time [85]. However, it has been shown that organic solvents that cause the PDMS to swell are able to remove

contaminants from the bulk allowing the surface to remain hydrophilic longer. It can remove uncrosslinked PDMS oligomers which would decrease the rotation of the carboxylic acids into the bulk [122].

Lastly, the application of *E. coli* attachment to PDMS surface can be explored. The first step in doing this would be to determine the optimum conditions for certain variables including changing the method as described above and eliminating the variable dealing with the PDMS. Next, the cells will need to be able to attach to the PDMS surface at a neutral pH to allow them to stay alive by changing the surface chemistry of the irradiated PDMS surface. A compound like a form of an amine or a protein could be attached to the carboxylic acids before being placed in the cell culture. By attaching a compound to the carboxylic acids, it forces them to not rotate back into the bulk polymer. Once the carboxylic acids are fixed, the *E. coli* could attach to the other compound. In order to determine if the bacteria were dead or alive, the cells could be transformed to produce the green fluorescent protein, GFP, which would fluoresce after being induced using IPTG. The dead cells could again be stained with propidium iodide. The alive cells would fluoresce the green color, but the dead cells would fluoresce green and red or a blue color. If the cells could be attached to the irradiated surface at a neutral pH then they could be incorporated into a microfluidic device as a possible biosensor. The BL-21 *E. coli* could be transformed to produce a type of detection if it came into contact with a specific solute.

References

[1] Kane, R. S.; Takayama, S.; Ostuni, E.; Ingber, D. E.; Whitesfield, G. M. Patterning proteins and cells using soft lithography. *Biomaterials*. **1999**, *20*, 2363-2376.

[2] Thomas, C.A.; Springer, P.A.; Loeb, G.E.; Berwald-Netter, Y.; Okun, L.M. A miniature microelectrode array to monitor the bioelectric activity of cultured cells. *Exp Cell Res*. **1972**, *74*, 61-66.

[3] Gross, G.W.; Rhoades, B.K.; Azzazy, H.M.E.; Wu, M.C. The use of neuronal networks on multielectrode arrays as biosensors. *Biosens Bioelec*. **1995**, *10*, 553-567.

[4] Jung, D.R.; et al. Cell-based microelectrode array characterized by imaging X-ray photoelectron spectroscopy, scanning electron microscopy, impedance measurements, and extracellular recordings. *J Vac Sci Technol A*. **1998**, 16, 1183-1188.

[5] Mrksich, M.; Whitesides, G.M. Patterning self-assembled monolayers using microcontact printing: a new technology for biosensors? *Trends Biotech*. **1995**, *13*, 228-235.

[6] Merritt, M.V.; Mrksich, M.; Whitessides, G.M, editors. Using self-assembled monolayers to study the interactions of man-made materials with proteins. *Principles of tissue engineering*. R. G. Landers Co.: Austin, 1997. 211-223.

[7] Fromherz, P.; Offenhausser, A.; Vetter, T.; Weis, J. A neuron-silicon junction: a Retzius cell of the leech on an insuated-gate field-effect transistor. *Science*. **1991**, *252*, 1290-1293.

[8] Mrksich, M.; Whitesides, G.M. Using self-assembled monolayers to understand the interactions of man-made surface with proteins and cells. *AnnRev Biophys Biomol Struct*. **1996**, *25*, 55-78.

[9] Singhyi, R.; et. al. Engineering cell shape and function. *Science*. **1994**, *264*, 696-698.

[10] Chen, C.S.; Mrksich, M.; Huang, S.; Whitesides, G.M.; Ingber, D.E. Geometric control of cell life and death. *Science*. **1997**, *276*, 1425-1428.

[11] Tang, L.; Min, J.; Lee, E.; Kim, J.S.; Lee, N.Y. Targeted cell adhesion on selectively micropatterned polymer arrays on a poly(dimethylsiloxane) surface. *Biomed Microdevices*. **2010**, *12*, 13-21.

[12] Leong, K.; Boardman, A.K.; Ma, H.; Jen, A.K.Y. Single-Cell Patterning and Adhesion on Chemically Engineered Poly(dimethylsiloxane) Surface. *Langmuir*. **2009**, *25*, 4615-4620.

[13] Veiseh, M.; Zhang, M. Effects of silicon oxidation on long-term cell selectivity of cell-patterned Au/SiO2 platforms. *J Am. Chem. Soc*. **2006**, *128*, 1197-1203.

[14] Ma, H.W.; Hyun, J.H.; Stiller, P.; Chilkoti, A. Non-fouling oligo(ethylene glycol)-functionalized polymer brushes synthesized by surface-initiated ATRP. *Adv. Mater*. **2004**, *16*, 338-341.

[15] Magani, A.; Priamo, A.; Pasqui, D.; Barbucci, R. Cell behaviour on chemically microstructured surfaces. *Mater. Sci. Eng. C* **2003**, *23*, 315-328.

[16] Ma. H.W.; Zhang, Z.; Beebe Jr., T.P.; Chilkoti, A. Fabrication of biofunctionalized quasi 3-dimensional microstructures of a nonfouling comb polymer by soft lithography. *Adv. Funct. Mater.* **2005**, *15*, 529-540.

[17] Iwanaga, S.; Akiyama, Y.; Kikuchi, A.; Yamato, M.; Sakai, K.; Okano, T. Fabrication of a cell array on ultrathin hydrophilic polymer gels utilizing electron beam irradiation and UV excimer laser ablation. *Biomaterials.* **2005**, *26*, 5395-5404.

[18] Duncan, A.; Rouais, F.; Lazare, S.; Bordenave, L.; Baquey, C.H. Effect of laser modified surface microtopochemistry on endothelial cell growth. *Colloids Surf. B.: Biointerfaces.* **2007**, *54*, 150-159.

[19] Hou, S.; Yang, K.; Qin, M.; Feng, X.Z.; Guan, L.; Yang, Y.; Wang, C. Patterning of cells on functionalized poly(dimethylsiloxane) surface prepared by hydrophobin and collagen modification. *Biosens. Bioelectron.* **2008**, *24*, 912-916.

[20] Xia, Y.; Whitesides, G.M. Soft Lithography. Angew. *Chem. Iru. Ed.* **1998**, *37*, 550-575.

[21] Kumar, A.; Biebuyck, H.A.; Whitesides, G.M. Patterning Self-Assembled Monolayers: Applications in Materials Science. *Langmuir.* **1994**, *10*, 1498-1511.

[22] Whitesides, G.M.; Kriebel, J.K.; Love, J.C. Molecular engineering of surfaces using self-assembled monolayers. *Science Progress.* **2005**, *88*, 17-48.

[23] Nuzzo, R.G.; Allara, D.L. Adsorption of bifunctional organic disulfides on gold surfaces. *J. Am. Chem.Soc.* **1983**, *105*, 4481-4483.

[24] Porter, M.D.; Bright, T.; Allara, D.L.; Chidsey, C.E. Spontaneously organized molecular assemblies. 4. Structural characterization of n-alkyl thiol monolayers on gold by optical ellipsometry, infrared spectroscopy, and electrochemistry. *J. Am. Chem. Soc.* **1987**,*109*, 3559-3569.

[25] Laibinis, P.E.; Whitesides, G.M. ω-Terminated alkanethiolate monolayers on surface of copper, silver, and gold have similar wettabilities. *J. Am. Chem. Soc.* **1992**, *114*, 1990-1995.

[26] Chidsey, C.E.D., Loiacono, D.N. Chemical functionality in self-assembled monolayers—structural and electrochemical properties. *Langmuir.* **1990**, *6*, 682-691.

[27] Lahann, J.; Mitragotri, S.; Tran, T.N.; Kaido, H.; Sundaram, J.; Choi, I.S; Hoffer, S.; Somorjai, G.A.; Langer, R. A reversibly switching surface. *Science.* **2003**, *299*, 371-374.

[28] McGovern, M.E.; Kallury, K.M.R.; Thompson, M. Role of solvent on the silanization of glass with octradecyltricholorsilane. *Langmuir.* **1994**, *10*, 3607-3614.

[29] Parikh, A.N.; Allara, D.L.; Azouz, I.B.; Rondelez, F. An intrinsic relationship between molecular structure in self-assembled n-alkylsiloxane monolayers and deposition temperature. *J. Phys. Chem.* **1994**, *98*, 7577-7590.

[30] Ulman, A. *An Introduction to Ultrathin Organic Films: From Langmuir-Blodgett to Self-Assembly.* Academic: London. 1991. Pg. 442.

[31] An, Y.H.; Friedman, R.J. Concise Review of Mechanisms of Bacterial Adhesion to Biomaterial Surfaces. *Journal of Biomedical Materials Research.* **1998**, *43*, 338-348.

[32] Cerf, A.; Cau, J.C.; Vieu, C. Controlled assembly of bacteria on chemical patterns using soft lithography. *Colloids and Surfaces B: Biointerfaces.* **2008**, *65*, 285-291.

[33] Mrksich, M. A surface chemistry approach to studying cell adhesion. *Chem. Soc. Rev.* **2000**, *29*, 267-273.

[34] Mrksich, M.; Dike, L.E.; Tien, J.; Ingber, D.E.; Whitesides, G.M. Using Microcontact Printing to Pattern the Attachment of Mammalian Cells to Self-Assembled Monolayers of Alkanethiolates on Transparent Films of Gold and Silver. *Experimental Cell Research.* **1997**, *235*, 305-313.

[35] Rozhok, S.; Shen, C.K.F.; Littler, P.L.H.; Fan, Z.; Liu, C.; Mirkin, C.A.; Holz, R.C. Methods for fabricating Microarrays of Motile Bacteria. *Small.* **2005**, *1*, 445-451.

[36] Frimat, J.P.; Menne, H.; Michels, A.; Kittel, S.; Kettler, R.; Borgmann, S.; Franske, J.; West, J. Plasma stenciling methods for cell patterning. *Anal Bioanal Chem.* **2009**, *395*, 601-609.

[37] Gan, J.; Chen, H.; Zhou F.; Huang, H.; Zheng, J.; Song, W.; Yuan, L.; Wu, Z. Fabrication of cell pattern on poly(dimethylsiloxane) by vacuum ultraviolet lithography. *Colloids and Surfaces B: Biointerfaces.* **2010**, *76*, 381-385.

[38] Berg, H.C. *E. coli in motion*; Springer-Verlag: New York, NY, 2004.

[39] Escherich, T. Die Darmbakterien des Neugeborenen und Sauglings. I. *Fortschr. Med.* **1885**, *3*, 515-522.

[40] Raetz, C. R. H.; Whitfield, C. Lipopolysaccharide Endotoxins. *Annu. Rev. Biochem.* **2002,** *71*, 635-700.

[41] Stevenson, G.; Neal, B.; Liu, D.; Hobbs, M.; Packer, N. H.; Batley, M.; Redmond, J. W.; Lindquist L.; Reeves, P. Structure of the O Antigen of *Escherichia coli* K-12 and the Sequence of Its *rfb* Gene Cluster. *Journal of Bacteriology.* **1994**, *176*, 4144-4156.

[42] Salton, M. J.; Kim, K.; Structure. In *Medical Microbiology*; 4th ed.; Baron, S., Ed.; University of Texas Medical Branch of Galveston: Galveston, TX, 1996.

[43] Mitik-Dineva, N.; Wang, J.; Truong, V.K.; Stoddart, P.; Malherbe, F.; Crawford, R.J.; Ivanova, E.P. *Escherichia coli, Pseudomonas aeruginosa,* and *Staphylococcus aureus* Attachment Patterns on Glass Surfaces with Nanoscale Roughness. *Curr Microbiol.* **2009**, *58*, 268-273.

[44] Mitik-Dineva, N.; Wang, J.; Mocanasu, R.C.; Stodart, P.R.; Crawford, R.J.; Ivanova, E.P. Impact of nano-topography on bacterial attachment. *Biotechnol. J.* **2008**, *3*, 536-544.

[45] Speranza, G.; Gottardi, G.; Pederzolli, C.; Lunelli, L.; Canteri, R.; Pasquardini, L.; Carli, E.; Lui, A.; Maniglio, D.; Brugnara, M.; Anderle, M. Role of chemical interactions in bacterial adhesion to polymer surfaces. *Biomaterials.* **2004**, *25*, 2029-2037.

[46] Orstavik, D. Sorption of *Streptococcus faecium* to glass. *Acta. Pathol. Microbiol. Scand.* **1977**, *85B*, 38-46.

[47] Abbot, A.; Rutter, P.R.; Berkeley, R.C.W. The influence of ionic strength, pH and a protein layer on the interaction between *Streptococcus mutans* and glass surfaces. *J. Gen. Microbiol.* **1983**, *129*, 439-445.

[48] Gordon, A.S.; Gerchakov, S.M.; Udey, L.R. The effect of polarization on the attachment of marine bacteria to copper and platinum surfaces. *Can. J. Microbiol.* **1981**, *27*, 698-703.

[49] Harber, M.J.; Mackenzie, R.; Asscher, A.W. A rapid bioluminescence method for quantifying bacterial adhesion to polystyrene. *J. Gen. Microbiol.* **1983**, *129*, 621-632.

[50] Van Loosdrecht, M.C.M.; Lyklema, J.; Norde, W.; Schraa, G.; Zehnder, A.J.B. Electrophoretic mobility and hydrophobicity in adhesion. *Appl. Environ. Microbiol.* **1987**, *53*, 1893-1897.

[51] Hogt, A.H.; Dankert, J.; de Vries, J.A.; Feijen, J. Adhesion of coagulase-negative staphylococci to biomaterials. *J. Gen. Microbiol.* **1983**, *129*, 2959-2968.

[52] Satou, N.; Satou, J.; Shintani, H.; Okuda, K. Adherence of streptococci to surface-modified glass. *J. Gen. Microbiol.* **1988**, *134*, 1299-1305.

[53] Baker, A.S.; Greenham, L.W. Release of gentamicin from acrylic bone cement: elution and diffusion studies. *J. Bone Joint Surg.* **1988**, *70A*, 1551-1557

[54] Howell, D.; Behrends, B. A review of surface roughness in antifouling coatings illustrating the importance of cutoff length. *Biofouling.* **2006**, *22*, 401-410.

[55] Scardino, A.J.; Harvey, E.; De Nys, R. Testing attachment point theory: diatom attachment on microtextured polyimide biomimics. *Biofouling.* **2006**, *22*, 55-60.

[56] Shellenberger, K.; Logan, B.E. Effect of molecular scale roughness of glass beads on colloidal and bacterial deposition. *Enviorn Sci Technol.* **2002**, *36*, 184-189.

[57] Chae, M.S.; Schraft, H.; Truelstrup, H. L.; et. al. Effects of physiochemical surface characteristics of *Listeria monocytogenes* strains on attachment to glass. *Food Microbiol.* **2006**, *23*, 250-259.

[58] LeVier, R.R.; Harrison, M.C.; Cook, R.R.; Lane, T.H. What is Silicone? *J. Clin. Epidemiol.* **1995**, *48*, 513-517.

[59] Campbell, D.J.; Beckman, K.J.; Calderon, C.E.; Doolan, P.W.; Ottosen, R.M.; Ellis, A.B.; Lisensky, G.C. Replication and Compression of Bulk and Surface Structures with Polydimethylsiloxane Elastomer. *Journal of Chemical Education.* **1999**, *75*, 537-541.

[60] Mark, J.E. Overview of Siloxane Polymers. In *Silicones and Silicone-Modified Materials*; Clarson, S.; et al., Ed.; ACS Symposium Series; American Chemical Society: Washington, DC, 2000; pp 1-10.

[61] Mark, J. E. Some Interesting Things about Poly siloxanes. *Accounts of Chemical Research.* **2004**, *37*, 946-953.

[62], H.; Gedde, U.W. Hydrophobicity Changes in Silicone Rubbers. *IEEE Transactions on Dielectrics and Electrical Insulation.* **1999**, *6*, 703-717.

[63] Graubner, V.M.; Jordan, R.; Nuyken, O.; Schnyder, B.; Lippert, T.; Kotz, R.; Wokaun, A. Photochemical Modification of Cross-Linked Poly(dimethylsiloxane) by Irradiation at 172 nm. *Macromolecules.* **2004**, *37*, 5936-5943.

[64] Owen, M.J.; Smith, P.J. Plasma treatment of polydimethylsiloxane. *J. Adhesion Sci. Technol.* **1994**, *8*, 1063-1075.

[65] Moon, M.W.; Vaziri, A. Surface modification of polymers using a multi-step plasma treatment. *Scripta Materialia.* **2009**, *60*, 44-47.

[66] Zhou, J.; Ellis, A.V.; Voelcker, N.H. Recent developments in PDMS surface modification for microfluidic devices. *Electrophoresis.* **2010**, *31*, 2-16.

[67] Mirley, C.L.; Koberstein, J.T. A Room Temperature Method for the Preparation of Ultrathin SiO_x Films from Langmuir-Blodgett Layers. *Langmuir.* **1995**, *11*, 1049-1052.

[68] Makamba, H.; Kim, J.H.; Lim, K.; Park, N.; Hahn, J.H. Surface modification of poly(dimethylsiloxane) microchannels. *Electrophoresis.* **2003**, *24*, 3607-3619.

[69] Hall, J.R.; Westerdahl, C.A.L.; Devine, A.T.; Bodnar, M.J. Activated gas plasma surface treatment of polymers for adhesive bonding. *Journal of Applied Polymer Science.* **1969**, *13*, 2085-2096.

[70] Hollahan, J.R.; Carlson, G.L. Hydroxylation of polydimethylsiloxane surfaces by oxidizing plasmas. *Journal of Applied Polymer Science.* **1970**, *14*, 2499-2508.

[71] Efimenko, K.; Wallace, W.E.; Genzer, J. Surface Modification of Sylgard-184 Poly(dimethyl siloxane) Networks by Ultraviolet and Ultraviolet/Ozone Treatment. *Journal of Colloid and Interface Science.* **2002**, *254*, 306-315.

[72] Berdichevsky, Y.; Khandurina, J.; Guttman, A.; Lo, Y.H. UV/Ozone modification of poly(dimethylsiloxane) microfluidic channels. *Sensors and Actuators B: Chemical.* **2004**, *97*, 402-408.

[73] Makamba, H.; Hsieh, Y.Y.; Sung, W.C.; Chen, S.H. Stable Permanently Hydrophilic Protein-Resistant Thin-Film Coatings on Poly(dimethylsiloxane) Substrates by Electrostatic Self-Assembly and Chemical Cross-Linking. *Analytical Chemistry.* **2005**, *77*, 3971-3978.

[74] Qui, J.; Hu, P.; Liang, R. Separation and Simultaneous Determination of Uric Acid and Ascorbic Acid on a Dynamically Modified Poly(dimethylsiloxane) Microchip. *Analytical Sciences.* **2007**, *23*, 1409-1414.

[75] Sui, G.; Wang, J.; Lee, C.C.; Lu, W.; Lee, S.P.; Leyton, J.V.; Wu, A.M.; Tseng, H.R. Solution-Phase Surface Modification in Intact Poly(dimethylsiloxane) Microfluidic Channels. *Anal. Chem.* **2006**, *78*, 5543-5551.

[76] Slentz, B.E.; Penner, N.A.; Lugowska, E.; Regnier, F. Nanoliter capillary electrochromatography columns based on collocated monolithic support structures molded in poly(dimethyl siloxane). *Electrophoresis.* **2001**, *22*, 3736-3743.

[77] Morra, M.; Ochiello, E.; Marola, R.; Garbassi, F.; Humphrey, P.; Johnson, D. On the Aging of Oxygen Plasma-Treated Polydimethylsiloxane Surfaces. *Journal of Colloid and Interface Science.* **1990**, *137*, 11-24.

[78] Yasuda, H.; Sharma, A.K. Effect of Orientation and Mobility at Surfaces on Contact Angle and Its Hysteresis. *J. Polm. Sci., Polym. Phys. Ed.* **1981**, *19*, 1285-1291.

[79] Vondracek, P.; Gent, A.N. Slow Decomposition of Silicone Rubber. *J. Appl. Polym. Sci.* **1982**, *27*, 4517-4523.

[80] Lee, C.L.; Homan, G. *Silicone Elastomer Protective Coatings for HV Insulators.* 1981 IEEE Conf. on Electrical Insulation and Dielectric Phenomena, Whitehaven, PA, USA, 1981, 435-443.

[81] Hillborg, H.; Gedde, U.W.; Hydrophobicity Recovery of Polydimethylsiloxane after Exposure to Corona Discharges. *Polymer.* **1998**, *39*, 1991-1998.

[82] Waddell, E.A.; Shreeves, S.; Carrell, H.; Perry, C.; Reid, B.A.; McKee, J. Surface modification of Sylgard 184 polydimethylsiloxane by 254 nm excimer radiation and characterization by contact angle goniometry, infrared spectroscopy, atomic force and scanning electron microscopy. *Applied Surface Science.* **2008**, *254*, 5314-5318.

[83] Schneemilch, M.; Quirke, N. Effect of oxidation on the wettability of poly(dimethylsiloxane) surface. *Journal of Chemical Physics.* **2007**, *127* (11), 114701.

[84] Williams, R.L.; Wilson, D.J.; Rhodes, N.P. Stability of plasma-treated silicone rubber and its influence on the interfacial aspects of blood compatibility. *Biomaterials.* **2004**, *25*, 4659-4673.

[85] Dharmarajan, P. Surface modification of polydimethylsiloxane by irradiation at 254 nm and effects on electroosmotic flow. M.S. Thesis, University of Alabama in Huntsville, Huntsville, AL, 2010.

[86] Minsky, M. Memoir of Inventing the Confocal Scanning Microscope. *Scanning.* **1988**, *10*, 128-138.

[87] Amas, W.B.; White, J.G. How the Confocal Laser Scanning Microscope entered Biological Research. *Biology of the Cell.* **2003**, *95*, 335-342.

[88] Roberts, F.; Young, J.Z. *The flying-spot microscope.* Proceeding of the IEE-Part IIIA: Televison. 1952, 99 (20), 747-757.

[89] Claxton, N.S.; Fellers, T.J.; Davidson, M.W. *Laser Scanning Confocal Microscope.* Tech rep.. National High Magnetic Field Laboratory. The Florida State University, Tallahassee, Florida 32390. 2006, 1-37.

[90] Pawley, J.B. *Handbook of Biological Confocal Microscopy*, 3rd ed.; Springer: New York, New York, 2006.

[91] Stelzer, E.H.K. Contrast, resolution, pixelation, dynamic range and signal-to-noise ratio: Fundamental limits to resolution in fluorescence light microscopy. *Journal of Microscopy.* **1998**, *189*, 15-24.

[92] Johnson, R. E.; Dettre, R. H. Wetting of Low-Energy Surfaces. In *Wettability*; Berg, J. C., Ed.; Marcel Dekker, Inc.: New York, New York, 1993.

[93] Jaycock, M. J.; Parfitt, G. D. *Chemistry of Interfaces*; Ellis Howard Ltd, Publishers: New York, New York, 1981; pg. 234-272.

[94] Zisman, W. A. Relation of the Equilibrium Contact Angle to Liquid and Solid Constitution. In *Contact Angle, Wettability, and Adhesion*, Vol. 43; Fowkes, F. M.; Ed.; American Chemical Society: Washington, D. C., 1964.

[95] Marmur, A. A Guide to the Equilibrium Contact Angles Maze. In *Contact Angle, Wettability, and Adhesion*, Vol. 6; Mittal, K. L., Ed.; Leiden: Boston Massachusetts, 2009.

[96] Good, R. J. Contact angle, wetting, and adhesion: a critical review. *J. Adhesion Sci. Technical.* **1992**, *12*, 1269-1302.

[97] Adamson, A. W. *Physical Chemistry of Surfaces*, 5th ed.; John Wiley & Sons: New York, New York, 1990.

[98] Kwok, D. Y.; Neuman, A. W. In *Surface Characterization Methods: Principles, Techniques, and Applications*; Milling, A. J., Ed.; Surfactant Science Series 87; Marcel Dekker: New York, New York, 1999.

[99] Young, T. Essay on the Cohesion of Fluids. *Philosophical Transactions of the Royal Society of London.* **1805**, *95*, 65-87.

[100] A. Dupre, Theorie Mecanique de la Charleur, Paris, 1869, pg 368.

[101] Gao, L.; McCarthy, T. J. Contact Angle Hystersis Explained. *Langmuir*, **2006**, *22*, 6234-6237.

[102] Pease, D. C. The Significance of the Contact Angle in Relation to the Solid Surface. *J. Phys. Chem.* **1945**, *49*, 107-110.

[103] Holmes-Farley, S.R.; Reamey, R.H.; McCarthy, T.J.; Deutch, J.; Whitesites, G.M. Acid-Base Behavior of Carboxylic Acid Groups Covalently Attached at the Surface of Polyethylene: The Usefulness of Contact Angle in Following the Ionization of Surface Functionality. *Langmuir.* **1985**, *1*, 725-740.

[104] Urban, M.W. *Attenuated Total Reflectance Spectroscopy of Polymers Theory and Practice.* In Polymer Surfaces and Interfaces Series. ACS: Washington, D.C.. 1996.

[105] Stuart, B.H. *Infrared Spectroscopy: Fundamentals and Applications*. John Wiley and Sons, Ltd., 2004.

[106] Alpert, N.L.; Keiser, W.E.; Szymanski, H.A. *IR Theory and Practice of Infrared Spectroscopy*, 2nd ed. Plenum Press: New York, New York, 1970.

[107] Harrick, N.J. Surface Chemistry From Spectral Analysis of Totally Internally Reflected Radiation. *J. Phys. Chem.* **1960**, *64*, 1110-1114.

[108] Fahrenfort, J. Attenuated total reflection: A new principle for the production of useful infra-red reflection spectra of organic compounds. *Sepctrochimica Acta*. **1961**, *17*, 698-709.

[109] Bardwell, J.A.; Dignam, M.J. Routine method for the determination of the optical constants of liquids. *Analytica Chimica Acta*. **1986**, *181*, 253-258.

[110] Molecular Probes. Propidium Iodide

[111] Jespras, R.I.; Carter, J.; Pearson, C.; Paul, F.E.; Wilkinson, M.J. Development of a Robust Flow Cytometric Assay for Determining Numbers of Viable Bacteria. *Applied and Environmental Microbiology*. **1995**, *61*, 2696-2701.

[112] P. Bouguer, *Essai d'optique sur la gradation de la lumière*. Gauthier-Villars et Cie, Paris 1729.

[113] J.H. Lambert, *Photometria sive de mensura et gradibus luminus, colorum et umbrae* (1760).

[114] A. Beer, Bestimmung der Absorption des rothen Lichts in farbigen Flüssigkeiten. *Annal. Phys. Chem.* **1852**, *86*, 78–88.

[115] Wrolstad, R. E. *Color and Pigment Analyses in Fruit Products*. Agricultural Experiment Station. 1976, Station Bulletin 624, 1-20.

[116] Perkampus, H.H. *UV-VIS Spectroscopy and Its Applications*; Springer-Verlag: New York, 1992.

[117] Rao, C. N. R. *Ultra-violet and Visible Spectroscopy Chemical Applications*; Plenu Press: New York, 1967.

[118] Wainright M.; Giddens, R. M. Phenothiazinium photosensitisers: choices in synthesis and application. *Dyes and Pigments*. **2003**, *27*, 245-257.

[119] Jockusch, S.; Turro, N. J.; Tomalia, D. A. Aggregation of Methylene Blue Adsorbed on Starburst Dendrimers. *Macromolecules*. **1995**, *28*, 7416-7418.

[120] A.F. Stalder, G. Kulik, D. Sage, L. Barbieri, P. Hoffmann, "A Snake-Based Approach to Accurate Determination of Both Contact Points and Contact Angles," *Colloids And Surfaces A: Physicochemical And Engineering Aspects*, vol. 286, no. 1-3, pp. 92-103, September 2006.

[121] Lambert, J. B.; Shurvell, H. F.; Lightner, D. A.; Cooks, R. G. *Organic Structural Spectroscopy*; Prentice Hall: New Jersey, 1998.

[122] Lee, J. N.; Park, C.; Whitesides, G. M Solvent Compatibility of Poly(dimethylsiloxane)-Based Microfluidic Devices. *Anal. Chem.* **2003**, *75*, 6544-6554.

APPENDIX

M9 minimal media recipe

For 500 mL, 1X M9, 1X glucose

- 3.4 g Na_2HPO_4
- 1.5 g KH_2PO_4
- 0.25 g NaCl
- 1 g dextrose
- 0.5 g NH_4Cl
- 5 mL divalents
- 1 mL vitamin B
- 5 μL trace elements
- Mix, sterile filter, and store in hood

Propidium Iodide recipe

Stock solution from solid

- Make a 1.5 mM concentrated solution using deionized water (1 mg/ mL)
- Store at 2-6°C, stable for 6 months

Working solution from stock solution

- Make a 1.5 μM working solution by diluting 1 μL of stock solution in 1 mL of PBS (1:1000).

Procedure for staining samples

- Pipet 300 μL of the working solution onto sample
- Cover with a glass coverslip
- Place sample with stain in a dark place for 30 minutes at room temperature
- Remove glass coverslip and rinse thoroughly with deionized water removing unbound dye
- Cover the sample with a new glass coverslip
- Sample is ready to be viewed which should be done immediately